FarmConners

Paving the Way for
Wind Farm Control in Industry

Recommendations for certification and standardisation of Wind Farm Control

Deliverable D2.3

Contents

Table 1: FarmConners report D2.3 author list

Authors	Organisation	Position	Contribution
Andreas Manjock	DNV Renewables Certification (RC)	Principal Engineer and Offshore Project Manager	Project Manager and WP2 Lead
Helena Canet	TUM	Phd Student	Contributing member
Filippo Campagnolo	TUM	Professor	Contributing member
Ervin Bossanyi	DNV Renewables Advisory (RA)	Senior Principal Engineer	Contributing member
Ricard Tomas bayo	DNV Renewables Certification (RC)	Principal Engineer	Contributing member
Thomas Duc	ENGIE GREEN	Development Engineer	Contributing member
Til Kristian Vrana	SINTEF Energy	Researcher	Contributing member
Konstanze Kölle	SINTEF Energy	Research Scientist	Contributing member
John Nwobu	ORE Catapult	R&D Engineer	Contributing member
Konstanze Kölle	SINTEF Energy	Research Scientist	Contributing member
Dr. Kai Freudenreich	DNV Renewables Certification (RC)	Principal Engineer	Contributing member

1 Executive Summary

Based on the position paper on certification and standardisation of Wind Farm Control (WFC), the FarmConners deliverable D2.1 [35], this report updates the recommendations for certification of WFC by making use of the results and developments of previous two years research work in the FarmConners project.

In Section 4 a load calculation with two different aero-servo-elastic simulations tools is presented covering three different wind turbine models (2.0MW-2.3MW-10MW). The time domain simulations considered extreme events during operation in wake steering mode and tried to identify the load impacts on turbine components due to WFC activities. A comparison with normal operation under extreme events (extreme turbulence, wind direction changes or shear) and under constrained wake steering modes has been performed. as a result a clear influence of wake steering operation on extreme load levels has been detected. The most significant ultimate limit state (ULS) load increase was found at wind speeds above rated wind speed and yaw misalignment angels greater $\pm 20°$.

Section 5 is looking firstly on the state-of-the-art wake modelling tools, partly further developed or improved in the Farm-Conners project, with special focus on the representation of wake effects under axial induction and wake steering modes. Then the theory and approach behind the farm flow simulation tool *LongSim* is presented. It covers several surrogate models and has been validated in the scope of the FarmConners project by a number of code-to-code comparisons. An exemplary flow simulation of a real offshore wind farm showed similar effects as found in the ULS sensitivity analysis, but here with respect to Fatigue limit States (FLS) loads. The pure wake steering strategy combined with a power optimised control configuration achieved the highest energy yield. However, this energy plus lead to a significant increase of damage equivalent loads (DEL's) on wind turbine component level.

Many load effects encountered in the ULS and FLS simulations could be qualitatively confirmed by field tests performed by FarmConners partner ENGIE GREEN a small wind farm in the north of France. The measurement campaigns between 2016 and 2021 included several axial induction modes and moderate wake steering modes. They are described in Section 6. Under application of axial induction modes a clear reduction of blade roots loads could be measured at the downwind turbine, but no noticeable power gain. Instead, under various wake steering modes a clear power output improvement could detected, but with increased blade loads at the same time (depending on the wake steering direction).

In Section 7 the perspective of the grid side on WFC influence is highlighted. WFC strategies could impact the standard grid code requirements on electric power quality, e.g. by voltage and frequency fluctuations. Also the capability to stabilise the grid during external faults should be maintained. On the other hand, WFC strategies allow to adjust the power performance of the entire farm according to electricity stock market prices and to offer and purchase further grid support services such as black start properties.

Finally, the load effects and the grid influences of WFC application are comprised and condensed to a set of recommendations for future certification procedures of WFC, outlined in Section 8. Recommendations for the preparation of certification documents (design basis) are given, followed by an approach for calculating an Independent Load Analysis (ILA) considering WFC strategies. A load case catalogue aligned with IEC and DNV standards has been amended by WFC considerations. With implementation of the recommendations into the next updates of certification standards (the update of the DNV-ST-0437 load standard is scheduled for 2022) a certification of wind turbines or wind farms using WFC is regarded feasible. Together with improved simulation tools and available certification formats a rapid increase of WFC's Technology Readiness Level (TRL) appears reasonable.

2   Introduction

This report reflects the research work of the FarmConners project with respect to the certification and standardisation of WFC strategies.

2.1   Basic WFC terminology

Wind farm control strategies have been explored in the last years with the perspective to improve power performance of wind farms. This new technology enables the improvement of the already excellent efficiency of modern wind turbines towards a further decrease of Levelised Costs of Energy (LCoE). With WFC strategies in place a wind farm can be operated very close like a conventional power plant with these main features:

- decrease or increase of power production on the short term and improvement of annual energy yield in the long term

- reduction of fatigue loading of individual turbines and corresponding reduction of maintenance costs and/or possible extension of the operational life time

- additional billable power system services (ancillary services) supporting the grid stability and possible power regulation according to electricity stock market prices

Since many different terminologies for WFC are still in use in the industry, research and literature, here a brief definition of terms used in this report is given.

Wind Farm Control (WFC) is the supervisory term for all control activities covering control activities from the control station down to the individual wind turbine controls. It comprises WPPC and WFFC.

Wind Power Plant Control (WPPC) is concerned with the connection to the power system and is responsible for compliance with grid codes and provision of power system services. This comprises the traditional way of operating a wind farm without consideration of aerodynamic turbine interaction.

Wind Farm Flow Control (WFFC) considers aerodynamic phenomena in the wind farm operation. It can be viewed as a new feature that shall be integrated with the existing control functions. In this report the WFC activities axial induction and wake steering are features controlled by WFFC.

Wind Turbine Control (WTC) implements the power set-points on the individual turbine and manage the optimal operational conditions. It comprises the safety & protection system which is independent from the operational control and is directly connected to mechanical sensors such as pitch failure sensors, overspeed detector or tower top vibration sensor

2.2   Basic certification levels

Certification of wind energy technology has been established in the wind industry since decades and provides confidence in technical integrity and reliability of wind energy assets. It supports investors and local authorities in the realisation of wind energy projects by third party expertise and confirmations.

The general intention of certification is to protect working personnel, assure functionality and structural integrity of systems and assets and to preserve the environment. Technically speaking these tasks correspond to a commonly agreed safety level. In the wind industry a safety level for operation of wind turbines has been defined by a target annual failure probability of $p = 10^{-4}$. In the recent wind energy standards this safety level is realised by safety factors, independent

calculations, tests, measurements, inspections and many other measures which allow to mitigate the technical risks towards the target safety level.

Below the most relevant certification modules for wind turbines are described in brief [53]. They are an extract of the description given in the service specification for project certification DNV-SE-0190 [18].

Concept Certification/Statement of Feasibility (SoF) can be achieved when completing the conceptual design stage of a wind farm control technology. It is usually based on a complete plausibility check of the conceptual design loads and of the conceptual design for all major wind turbine components. For wind farm control it is furthermore based on the control and safety concept which comprises relevant wind farm control aspects. Depending on the complexity of the new wind farm control technology provided by a supplier, a qualification program (Technology Qualification according to DNV-RP-A203 [16]) can be performed to individually establish the necessary steps for verification e.g. towards a prototype certification.

Type certificate (TC) covers the third-party verification of design, testing and manufacturing of a component or a software in serial production and for multi-purpose application. In the wind industry it is common practice that the wind turbine types own a type certificate according to IEC or DNV standards. With regards to wind farm control, the type certificate covers the compatibility of the wind turbine for a range of predefined wind farm control strategies. The assessment includes an independent load calculation including wind farm control specific design load cases, a verification of the wake and load model validation performed and comparison with tests. Generic conditions are considered to cover the expected ranges for site-specific parameters the wind farms shall be erected in later on (see Site Specific Design Assessment). Verification of the wind turbine structural components is an inherent part of the design assessment. Further assessments comprise the safety and control system as well as the electrical system complimented by wind farm control related features. In this context DNV-ST-125 "Grid code compliance" [22] will be applied in order to check if changes in electrical power initiated by wind farm control negatively impact typical GCC-features of the wind turbine.

Site Specific Design Assessment (SSDA) of a wind farm applying wind farm control features proves that its design is fit for application in the site specific environment considering specific wind farm related parameters like individual wind conditions, turbine layout and wake effects applying wind farm control features at the same time. It is based on an existing type certificate for the individual wind turbines while site-specific load assumptions considering the effects of wind farm control and a potential impact of the electrical grid on the loads are assessed. This replaces any generic assumptions made in the type certificate. Wind farm control-related design changes, e.g. regarding the control and protection system or the electrical components, are addressed which have not been considered in the type certification before. A measurement campaign according to section 8.13 in DNV-SE-0190 [18] can reduce the uncertainty associated with the application of new load simulation approaches for wind farm control.

Project certificate (PC) is successfully completed if a system or asset is regarded proven in an operational environment. For the planning, the installation and the operation of a wind farm applying the project certification is recommended. It stipulates that the risks arising from site assessment, design basis, design, manufacture, transport, installation, commissioning, operation and maintenance are considered. The project certificate incorporates the SSDA to address wind farm control related design features.

The following figure illustrates the application of the different certification modules.
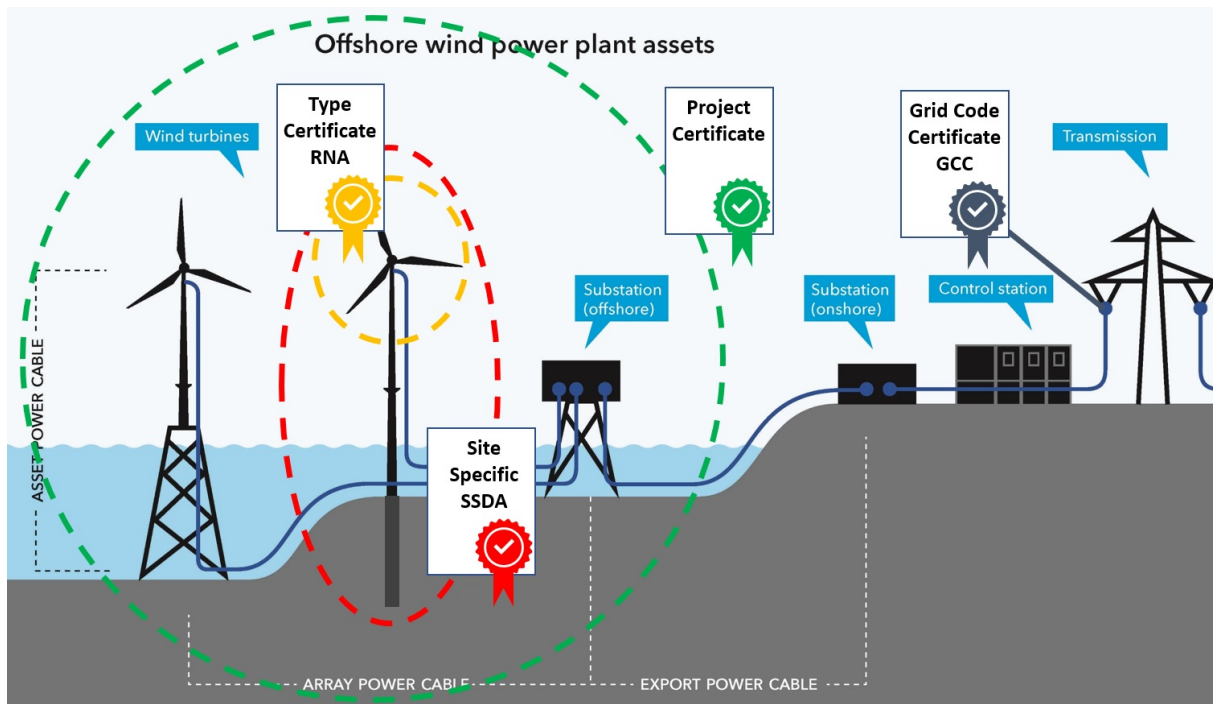
Figure 1: Offshore wind power plant assets according to DNV-SE-0190 [18]

It should be mentioned the Project Certificate covers the assets array power cable, substation, export power cable and control station optionally. The Grid Code Compliance certificate is a separate assessment at the Point of Connection (PoC) and applies DNV-ST-0125 [22] in combination with local grid code requirements.

3   Update on regulatory landscape

A first overview on the existing guidelines and standards related to wind farm control has been provided in the FarmConners deliverable D2.1 Position paper on certification, standardisation, and other regulatory issues of Wind Farm Control [35]. For the certification of wind farms, either the DNV scheme or the IECRE scheme applies.

In the IECRE-OD-502 [38] WFC is mentioned in section 7.2 "Project design basis evaluation" as well as in the related figures 1 and 2. It is part of the list of optional items, which can be included in the project design basis. Requirements specific to WFC are not given.

The DNV-SE-0190 section 8.13 "Wind farm control" [18] describes requirements on the certification of WFC. An empirical procedure is outlined how to include WFC into an SSDA and how to proceed, if the tools used for simulation of WFC specific loads are not validated yet.

Thus, in both certification specifications there is a reference to wind farm control certification. However, in both specifications there is no clear guidance given about how Wind Farm Control (WFC) should be performed in detail.

3.1   Empirical approach combined with provisional certification

The service specification DNV-SE-0190 is the most recent updated certification scheme with respect to WFC.

A validation of WFC application could be carried out during operation of the (commercial) wind power plant under investigation. During the Site-Specific Design Assessment (SSDA) the new or modified models for determination of external conditions and simulation of load simulations are only assessed on a plausibility basis, but not finally approved. The issued SSDA includes conditions, that the validity of the new modules shall be approved by measurements during the first years of operation of the realised wind farm. This is based on a measurement plan to monitor first years of wind farm operation and yearly reports on the wind farm control performance and data acquisition. If these measurements (external conditions, loads, SCADA data, etc.) show that all new models and tools have determined correct calculations, an unconditioned SSDA will be issued. In case the new models have underpredicted the loads, the realistic loads must then be calculated based on the measured values. Load mitigation procedures must be applied to the plant, e.g. by curtailment to meet the initially planned lifetime.

3.2   Further certification alternatives

As an alternative to the empirical certification approach mentioned above, the DNV service specification for project certification proposes a risk based certification approach. By applying a Failure Mode Effect and Criticality Analysis (FMECA) the potential risks of a WFC application could be identified by employing the systematic process of a Technology Qualification as described in [17], [16], [20] or [21]. The result is a tailored action plan to mitigate the identified risks of the WFC concept.

Furthermore, another DNV standard is under revision which explicitly considers WFC. The standard DNV-ST-0437 "Loads and site conditions for wind turbines" will include a separate section on certification of WFC strategies [23] and is scheduled for end of 2022.

4 Load effects of WFC strategies on wind turbine level

Wake steering strategies are generally adopted to maximise the power production of a wind farm. These strategies assign large yaw misalignment set points to a number of selected wind turbines of the wind farm. These large yaw misalignments required by wake steering are so far not considered in the design standards and are therefore, off-design conditions. While the benefits of wake steering strategies in annual Energy production (AEP) are being widely researched, the impact of these strategies in the structural safety of current wind turbines and the possible implications in their design are not fully understood and validated. This chapter aims at taking a first small step to bridge this gap and investigates the impact of large yaw misalignments on extreme loads, based on numerical simulations, for different power production operating cases. The study aims at giving a rough preliminary answer to the following three main questions:

- What is the impact of large yaw misalignments occurring coincidentally with extreme environmental events during power production?

- Which operating ranges – in terms of wind speed and yaw misalignment – are safe for turbines designed with the current standards?

- Which components in particular are more affected by extreme yaw misalignment operation?

Clearly, the impact of yaw misalignment in extreme loads will depend on the aerodynamic models implemented in the simulation tool, as well as the characteristics and specific design drivers of the wind turbine analyed. This study therefore considers two different aero-servo-elastic simulators and three different reference wind turbines, which differ for wind class, size and power rating. These three reference machines are widely used for academic studies and are considered to be reasonable approximations of current wind turbines available on the market.

The chapter is structured in five sections. Section 4.1 describes the aero-servo-elastic solvers and controllers used for the load analysis presented in this chapter. Section 4.2 characterises the extreme loads in power production of a reference machine. The simulations are performed with two different aero-servo-elastic simulators, *Cp-Lambda* and *Bladed*. Section 4.3 repeats the study for two additional reference machines. The impact of yaw misalignment in extreme loads for the three reference machines is here compared. Finally, Section 4.4 gives a final overview of the conclusions and lists the limitations of the study here presented.

4.1 Tool description for coupled analysis

The two aeroserovelastic tools employed are *Bladed* and *Cp-Lambda*, and are described as follows.

4.1.1 Bladed

Bladed is a DNV code for hydro-aero-servo-elastic load simulations in time domain, originally developed by Garrad Hassan. Time domain simulations are necessary for non-linear, dynamic and transient processes, which are important for the load analysis of modern large wind turbines. The aerodynamic forces are calculated with the blade element momentum theory (BEMT) [15]. Although the BEM theory is not fully valid for large 3-dimensional flow conditions over the the rotor blade surface the approach is considered acceptable for the qualitative purpose of this sensitivity study. In addition, the code is able to simulate a wake behind the rotor and dynamic stall. The calculation of rotor loads has been validated against numerous certification measurements and research projects, see e.g. [55] and [13]. During the coupled simulation *Bladed* calculates the structural dynamics with a multibody-dynamic-approach. The components such as blades, tower and foundation are modelled with flexible elements whose deformation is determined by modal analyses. This is

done by a linear combination of the calculated eigenmodes resulting from a Finite Element Method (FEM) calculation. The tower module gives the possibility to introduce a stiffness representation to each structural member (Timoshenko beam model). This allows a load simulation of the tower and foundation with consideration of a fully flexible structure. This allows the modelling of very complex structural dynamics under consideration of the fully coupled interaction between stochastic environment, non-linear control algorithms and flexible structural elements. With the statistical tool box of *Bladed* the post-processing of simulated time series allows to produce Ultimate Limit States (ULS), Fatigue Limit States (FLS) and Accidental Limit States (ALS) at any defined node of the wind turbine. Beside the these outputs *Bladed* includes a wide set of engineering and scientific analysis methods.

4.1.2   Cp-Lambda

The aero-servo-elastic multibody-based code *Cp-Lambda* (Code for Performance, Loads, Aeroelasticity by Multi-Body Dynamic Analysis) is used as the second coupled analysis tool in this study. The code, originally developed for rotorcraft applications, is based on Cartesian coordinates and scaled Lagrange multipliers for the enforcement of constraints, while it performs the forward time integration by an implicit nonlinearly unconditionally stable energy decaying scheme. *Cp-Lambda* implements a complete library of elements, including nonlinear flexible composite-ready beams, rigid bodies, joints, actuators and sensors. The code is tightly coupled with aerodynamic models based on the classical blade element momentum (BEM) approach, formulated according to the annular stream-tube theory with wake swirl, including tip and hub loss models, as well as unsteady corrections and dynamic stall. Turbulent wind time histories are generated with the open-source code *TurbSim* [40] while deterministic gusts are generated according to international standards. *Cp-Lambda* has been used in several industrial and research projects, and it has been validated against industrial simulation programs, wind tunnel experimental results and field measurements. Readers interested in the mathematical formulation of *Cp-Lambda* can refer to the references [7, 12, 6]. The wind turbine model is interfaced with an external routine, implementing the necessary supervision and control strategies. In the current study, the linear quadratic regulator (LQR) described in [11] was used, while the yawing mechanism is driven by a yaw controller with a simple logic.

4.2   Study of the DTU 10 MW machine

The DTU 10 MW [8] is a reference machine of 178.3 m rotor diameter and a hub height of 119 m. An overview of the characteristics of this machine is given in Tab. 2. This turbine has been widely used for several studies and will be here used to investigate the impact of large yaw misalignment on extreme loads with the two different aero-servo-elastic simulators, namely *Cp-Lambda* and *Bladed*.

	DTU 10MW Turbine 1 [8]
IEC Class & Category	2A
Rated electric power [MW]	10
Rotor diameter [m]	178.3
Specific power [W/m^2]	400.5
Hub height [m]	119.0
Blade mass [t]	42.50
Tower mass [t]	617.5

Table 2: Description of the DTU 10 MW machine [8]

First, the reference machine is modelled with *Cp-Lambda* and *Bladed*, the two aero-servo-elastic simulators described inSection 4.1. The performance of these two models is compared inSection 4.2.1, where sources of divergences are also

highlighted. Finally,Section 4.2.2 analyses and compares the impact of yaw misalignment in different load sensors.

4.2.1 Model alignment of the two simulation codes

Figure 2 compares the natural frequencies of the reference turbine modelled with *Cp-Lambda* with the natural frequencies of the *Bladed* model. Results show a good matching for the tower fore-aft and side-side frequencies, with a maximum difference of 1%. The blade natural frequencies of the *Cp-Lambda* model are also found to follow well the *Bladed* model, with a maximum difference of about 1.5% in the first flapwise frequency.
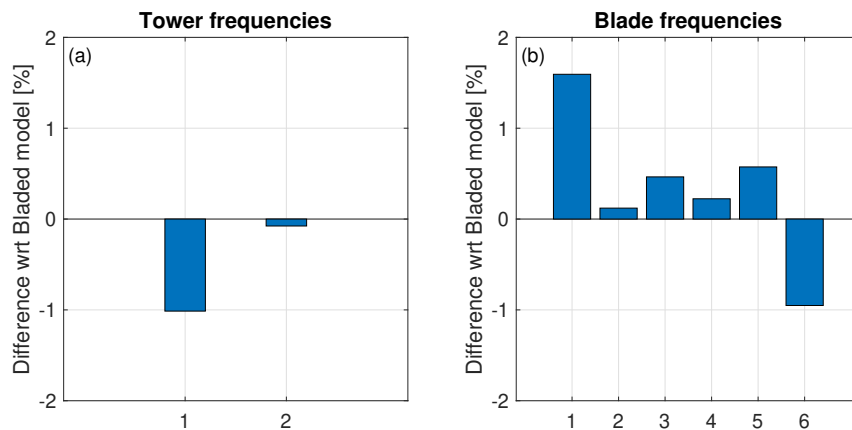

Figure 2: Comparison between the (a) tower and (b) blade natural frequencies of the *Cp-Lambda* DTU 10 MW model with respect to the *Bladed* DTU 10 MW model

Additionally, the distribution of different load sensors is also compared. Figure 3 shows the performance of the maximum value of these load sensors at each wind speed. The study focuses here on flapwise blade root moment (FBRM), torque, combined moment at tower bottom (CMTB) and torsion moment at tower top (TMTT). Result shows that the *Cp-Lambda* model follows the *Bladed* model well in FBRM and CMTB. A different trend is observed for Torque (Figure 3b) and TMTT (Figure 3d) due to differences in the logic of the pitch-torque controller.

It should be here as well noted, that differences also arise from the different turbulent models considered. Indeed, while both models are simulated for a turbulence category B, *Bladed* considers Mann spectrum, while the *Cp-Lambda* simulations are performed considering a Kaimal turbulence model.

4.2.2 Study of the 10 MW reference machine in yawed conditions

Next, a set of simulations is run with each aero-servo-elastic model to analyse the impact of large yaw misalignment. Table 3 lists all the design load cases considered in this study. Each DLC here listed is simulated for 15 different yaw misalignments, from -38 degrees to +38 degrees. Each simulation is run with 6 seeds in the case of *Cp-Lambda*, and 12 seeds for the simulations run with *Bladed*.
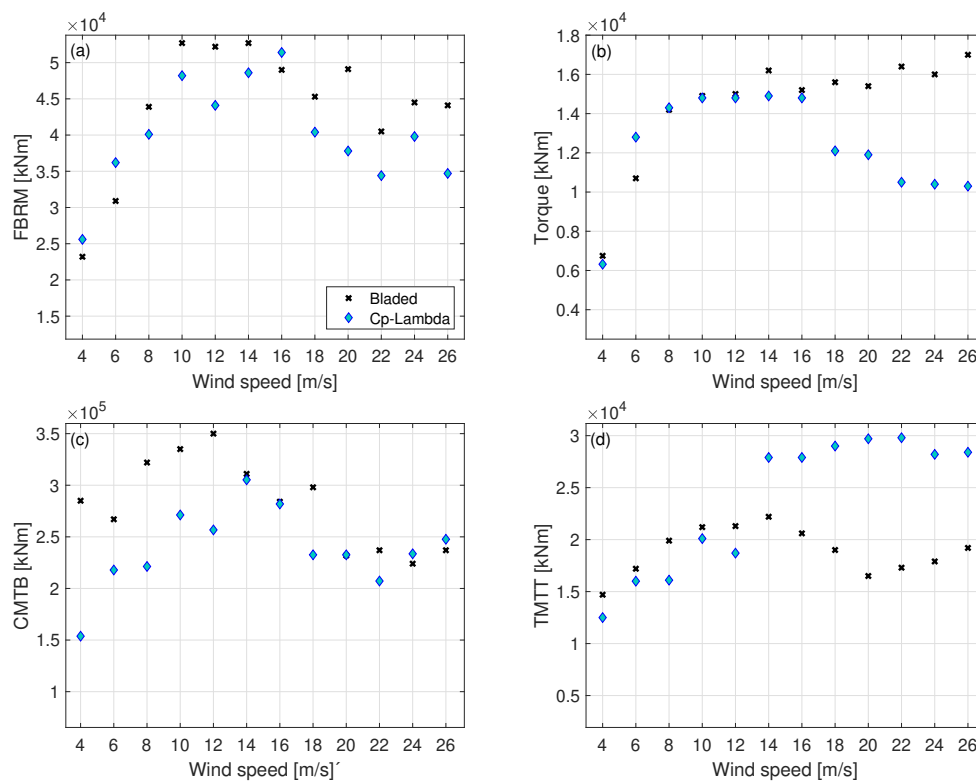
Figure 3: Comparison between selected load sensors, where FBRM is the flapwise blade root moment; CMTB is the combined moment at tower bottom and TMTT is the torsion moment at tower top.
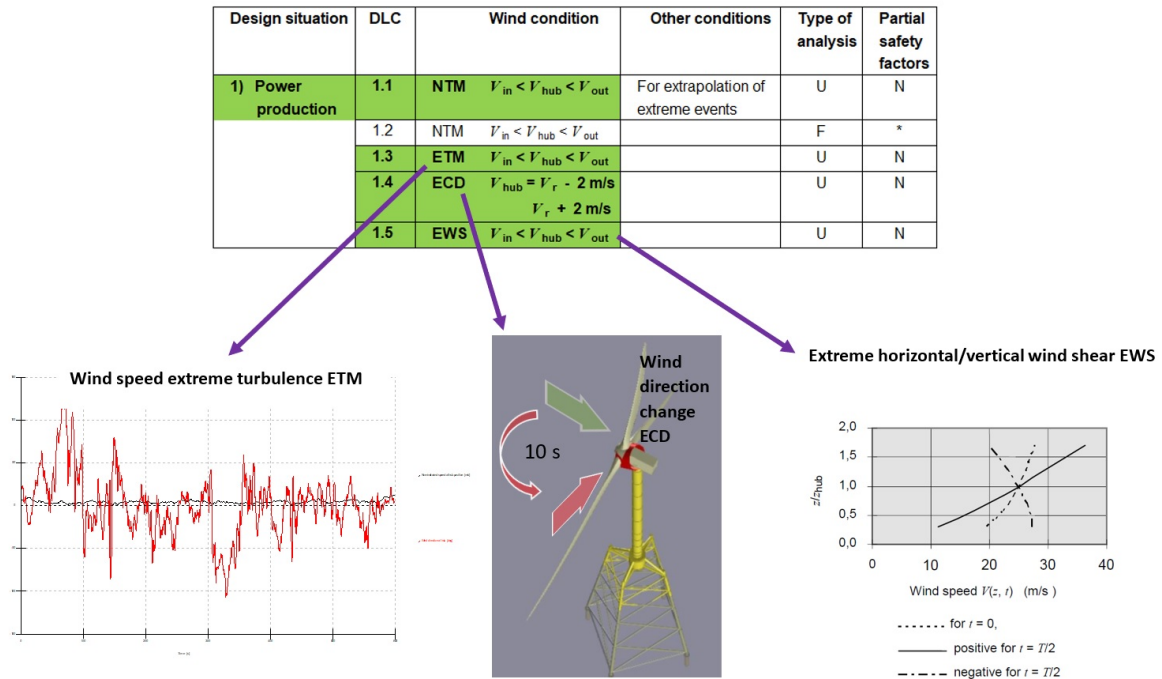
Design situation	DLC	Wind condition		Other conditions	Type of analysis	Partial safety factors
1) Power production	1.1	NTM	$V_{in} < V_{hub} < V_{out}$	For extrapolation of extreme events	U	N
	1.2	NTM	$V_{in} < V_{hub} < V_{out}$		F	*
	1.3	ETM	$V_{in} < V_{hub} < V_{out}$		U	N
	1.4	ECD	$V_{hub} = V_r - 2$ m/s $V_r + 2$ m/s		U	N
	1.5	EWS	$V_{in} < V_{hub} < V_{out}$		U	N

Figure 4: ULS load cases applied

DLC	Design situation	Wind speed	Wind profile	Yaw misalignment [deg]
1.1	Power production	$V_{in}{:}V_{out}$	NTM	$\pm38, \pm30, \pm25, \pm20, \pm15, \pm10, \pm8, 0$
1.3	Power production	$V_{in}{:}V_{out}$	ETM	$\pm38, \pm30, \pm25, \pm20, \pm15, \pm10, \pm8, 0$
1.4	Power production	$V_{rated} \pm 2$ m/s	ECD	$\pm38, \pm30, \pm25, \pm20, \pm15, \pm10, \pm8, 0$
1.5	Power production	$V_{in}{:}V_{out}$	EWS	$\pm38, \pm30, \pm25, \pm20, \pm15, \pm10, \pm8, 0$

Table 3: Design Load Cases considered in this study. NTM = Normal turbulence model; ETM = Extreme turbulence model; ECD = Extreme coherent gust with direction change; EWS = Extreme wind shear; EOG = Extreme operating gust; EWM = Extreme wind speed model.

The analysis focuses on nine different load sensors: torsion blade root moment (TBRM), flapwise blade root moment (FBRM), edgewise blade root moment (EBRM), tower clearance (TC), torque, thrust, fore-aft moment at the tower top (FAMTT), side-side moment at tower top (SSMTT) and combined moment at tower bottom (CMTB). Figure 5 displays the maximum value of each load sensor for each DLC. The results here shown correspond to the values obtained with the *Cp-Lambda* model, however similar trends are obtained for the *Bladed*, not shown here to avoid redundancy. Clearly, DLC1.3 is the design load case responsible for the maximum values for all load sensors. It should be additionally remarked, that only DLC1.1 and DLC1.3 actually consider realistic turbulent conditions. Indeed, the wind profiles prescribed by the standards for DLC1.4 and DLC1.5 are *artificially* created to represent potential events in the lifetime of a wind turbine, but do not represent real conditions. The validity of adding a yaw misalignment in these conditions should therefore be further explored.

Next, the study compares the trends obtained with each aero-servo-elastic solver for different load sensors of the DTU 10 MW reference turbine model. The trends obtained are shown in Figure 6, where the left column shows the trends
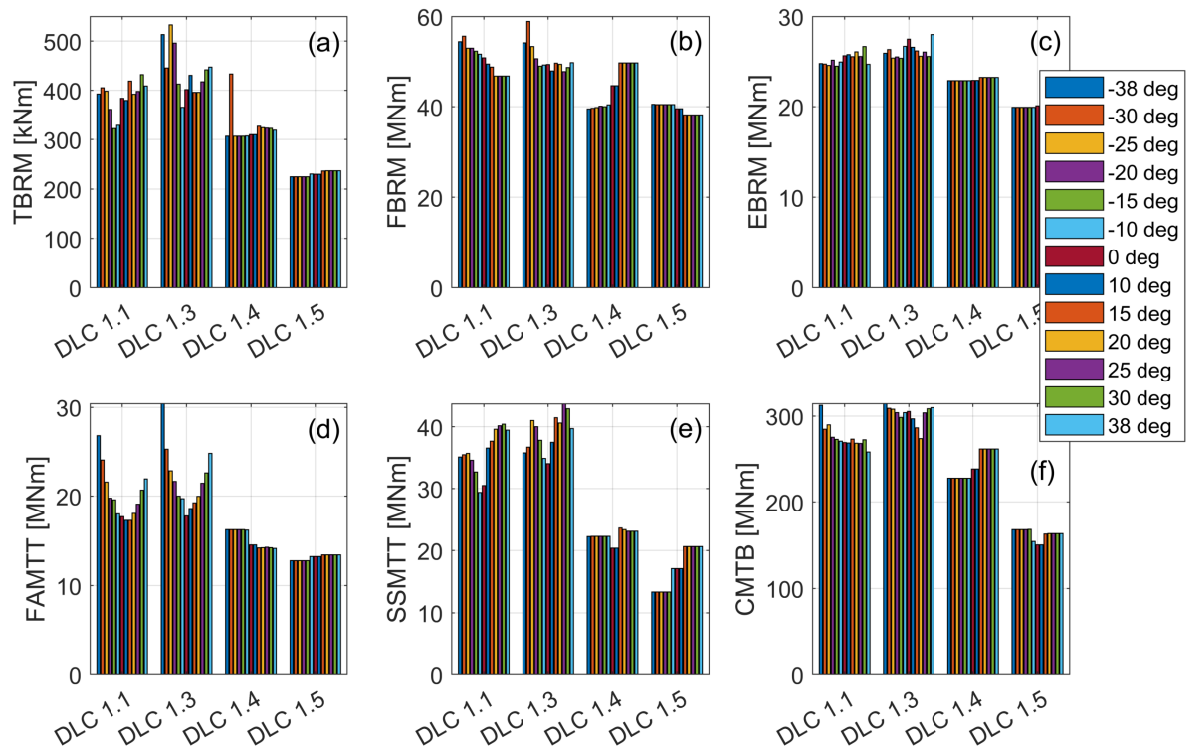
Figure 5: Maximum (a) torsional blade root moment (TBRM); (b) flapwise blade root moment (FBRM); (c) edgewise blade root moment (EBRM); (d) fore-aft moment at tower top (FAMTT); (e) side-side moment at tower top (SSMTT); (f) combined moment at tower bottom (CMTB) for the considered DLCs and yaw misalignment conditions, for the DTU 10 MW machine modelled with *Cp-Lambda*

per wind speed obtained with *Cp-Lambda*, while the right column shows the results for *Bladed*. Each boxplot contains all extreme values of the load sensor of interest obtained for each blade (or tower for CMTB). Only the DLC1.3 cases are here considered and they are divided into two operating conditions:

- The continuous line correspond to the value at the 95% quantile.

- Operation under normal yaw misalignment (black line): includes operation with $\pm 8°$ and $0°$ yaw misalignment

- Operation under extreme yaw misalignment (red line): includes operation with $\pm 10°$, $\pm 15°$, $\pm 20°$, $\pm 25°$, $\pm 30°$ and $\pm 38°$ yaw misalignments.

Figure 6a and Figure 6b show a similar trend for blade root flapwise bending moment (FBRM) between the two models, with the *Bladed* model showing slightly higher values for both normal and extreme yawed operation. Both models show the same trend: Maximum blade root flapwise bending moment remains equal for normal and extreme yawed conditions around rated wind speed (12 m/s). A higher blade root flapwise bending moment is obtained for yawed conditions after rated speed. Figure 6c and Figure 6d compare the trend for the blade root edgewise bending moment (EBRM) between the two models. In this case, the *Bladed* model presents lower values than the *Cp-Lambda* model. The same trend between normal and extreme yawed conditions is observed, with blade root edgewise bending moment not presenting any significant increase until rated wind speed. The impact of yaw misaligned operation in tower clearance (TC) is investigated in Figure 6e and Figure 6f. Results show here a good matching between the blade deflections of the two models and a decrease of tower clearance after rated speed. Finally, Figure 6g and Figure 6e compare the impact of yaw misaligned operation at combined tower bottom bending moment (CMTB). For this load sensor, the *Bladed* model shows slightly higher values than the *Cp-Lambda* model. Both models show a larger impact of yaw misaligned operation beyond rated wind speed.

Finally, the trends displayed in Figure 6 are quantified through safety coefficients, defined here for a load sensor as the ratio between the maximum value of this load sensor for operation in normal yaw misalignment, and the maximum value of the same load sensor for operation in extreme yaw misalignment. Additionally, based on the trends observed in Figure 6, four scenarios are defined:

- **All cases:** This scenario considers the complete range of yaw misalignment analysed (from -38° to +38°) and all wind speeds.

- **Wind speed-constrained:** This scenario considers the complete range of yaw misalignment analysed (from -38° to +38°), and only wind speeds up to rated wind speed. No yaw misalignment is considered after rated wind speed.

- **Yaw-constrained:** This scenario considers a partial range of yaw misalignment (from -25° to +25°), and all wind speeds.

- **Wind speed- and yaw-constrained:** The two scenarios described above are combined: this scenario considers a partial range of yaw misalignment (from -25° to +25°), which is similar to the current capabilities of yaw actuators, but only wind speeds up to rated wind speed. No yaw misalignment is considered after rated wind speed.

Figure 7 compares the safety coefficients obtained for each model and each scenario. Clearly, safety coefficients decrease when both wind speed and yaw misalignment range are constrained. Figure 7d shows that most of the load sensors present zero or negligible increases. Only the safety coefficient for FAMTT is clearly higher for both *Cp-Lambda* and *Bladed*. This load sensor however, only considers the fore-aft moment and therefore does not have significant implications for the structural safety of the tower. Additionally, tower clearance is also slightly higher than 1 for both *Bladed* and *Cp-Lambda*. Understanding the implication of this increase for the blade structural safety (or the design of the blade) is not straightforward, as this quantity measures the available distance between the deflected blade and the tower surface, but does not assess this distance, i.e. it is not known if the blade would strike the tower.
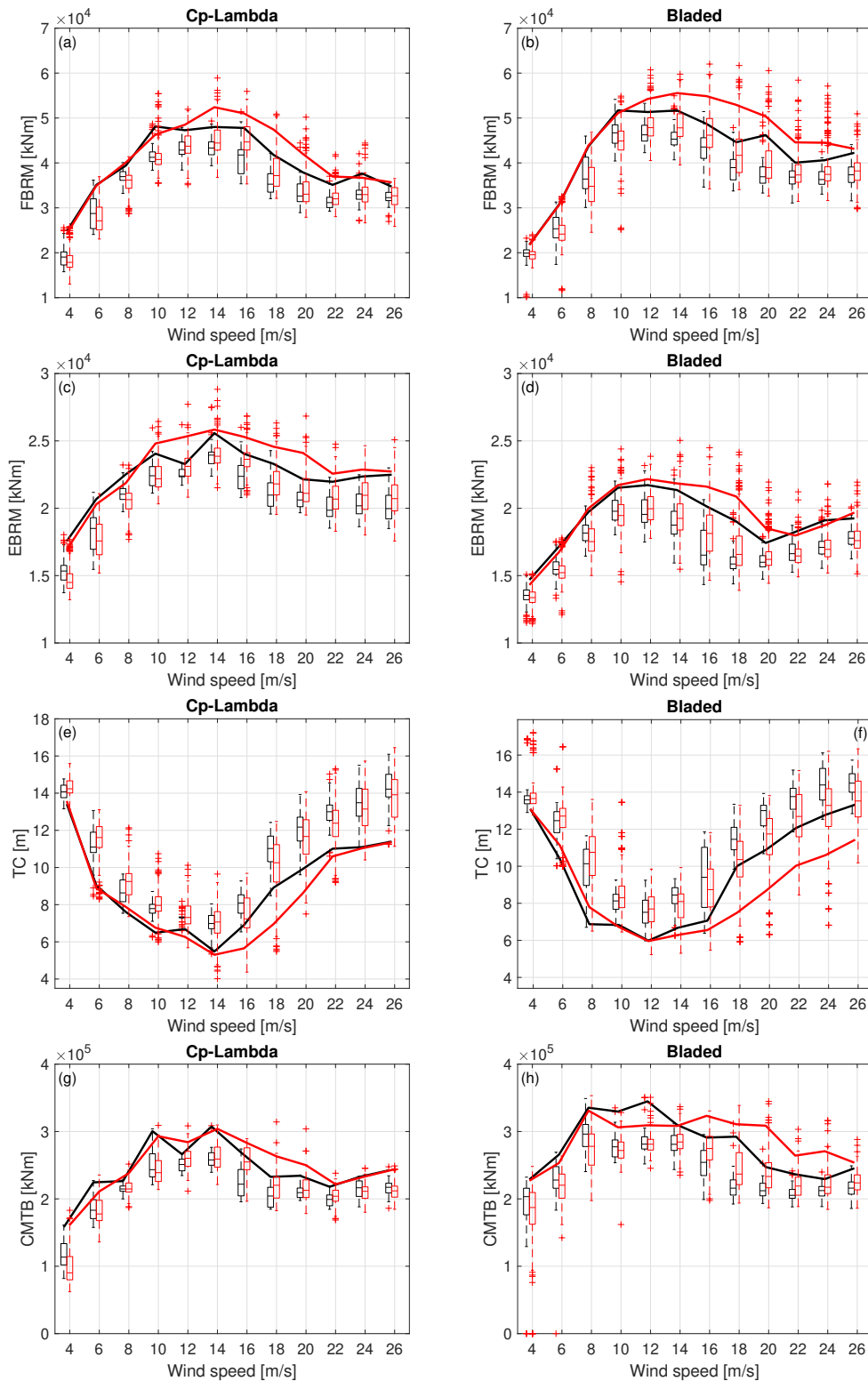
Figure 6: Comparison of load trends for FBRM, EBRM, TC and CMTB, simulated with *Cp-Lambda* (left column) and *Bladed* (right column). Yaw misalignment are aggregated in two different categories: normal yaw conditions (±8°, 0 degrees, black line) and extreme yaw conditions (±10°, ±15°, ±20°, ±25°, ±30° and ±38°). Continuous line corresponds to the 95% quantile.
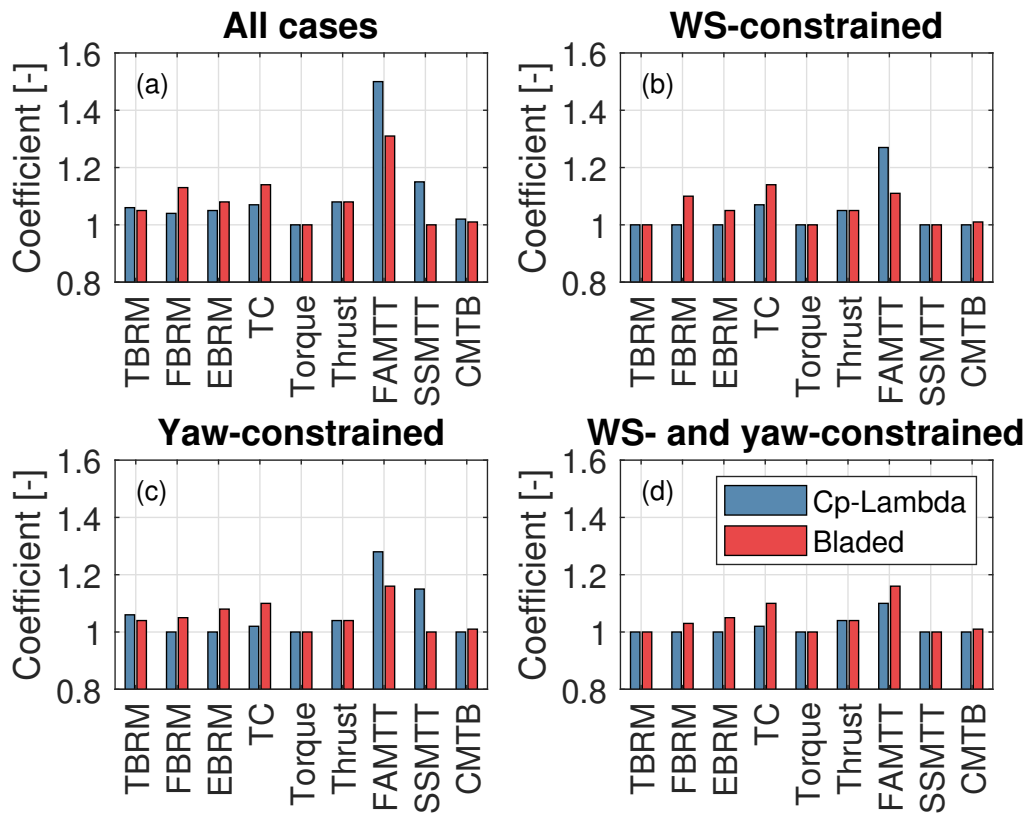
Figure 7: Comparison between the safety coefficients obtained with *Cp-Lambda* and *Bladed*, for the different scenarios considered (see text)

4.3 Sensitivity analysis: Analysis of reference turbines of different specific power/class

This section extends the study presented inSection 4.2 with two additional machines. This study is performed with only one aero-servo-elastic simulator, *Cp-Lambda*.

4.3.1 Description of the 2.2 MW and the 3.35 MW reference turbines

The study is repeated for two additional wind turbines: a 2 MW machine [9] and the land-based IEA Wind Task 37 3.35 MW [10] reference turbine. Table 4 shows the main characteristics of these two reference machines. These machines differ in terms of specific power and class.

	Turbine 2 [9]	Turbine 3 [10]
IEC Class & Category	2A	3A
Rated electric power [MW]	2.2	3.35
Rotor diameter [m]	92.4	130.0
Specific power [W/m^2]	298.3	252.4
Hub height [m]	80.0	110.0
Blade mass [t]	8.62	16.44
Tower mass [t]	125	553

Table 4: Description of the two machines used for the sensitivity analysis

4.3.2 Study of the machines in yawed conditions

The study considers here as well the design load cases described in Table 3. For these machines, DLC1.3. is also found to be the design load case driving the extreme loads for the load sensors considered and therefore, the focus of this study. Figure 8 gives an overview of the impact of extreme yaw misaligned operation for the three different machines and four selected load sensors. The relative difference between the maximum value of operation under extreme yaw misalignment with respect to the maximum value of operation under normal yaw misalignment is here computed for each wind speed, and each reference machine. Figure 8a shows a similar pattern for the three turbines, with larges increases in torsional blade root moment (TBRM) under rated wind speed, and a less significant impact in higher wind speeds. Figure 8b shows the impact in FBRM, a load which presents a higher value after rated wind speed for the three reference models. The reduced impact of yaw misalignment in this load sensor, as well as the different rated speed of the three reference models difficult the visualisation of a clear trend. A similar conclusion can be taken for EBRM, which presents larger values after rated wind speed, but the reduced impact in some of the models makes it difficult to spot a clear trend (Figure 8c. Finally, CMTB (8d), the combined moment at tower bottom clearly increases after rated wind speed for the three models, but also presents slightly higher values under rated wind speed.

Finally, the trends displayed in Fig 8 are quantified through safety factors, as defined inSection 4.2.2. Here again, four scenarios are defined based on the trends observed. CMTB is the load sensor with the largest safety factor, if all wind speeds and yaw misalignments are considered (Fig 8a). This load sensor, however, is reduced to 1 when the yaw of the turbine is misaligned only under rated wind speed. A similar trend is seen for the other key quantitiy relative to the tower, CMTT, even if the initial impact is here lower. The safety factors of the load sensors relative to the blade (TBRM, FBRM, EBRM) also significantly benefit from the reduced range of wind speeds and yaw misalignments. Clearly, only the safety factor of TBRM is higher than 1 for two of the three reference machines in the most restrictive scenario. The study shows that, even if a general trend can be seen for the load sensors considered, the specific safety factors depend on the turbine analysed.
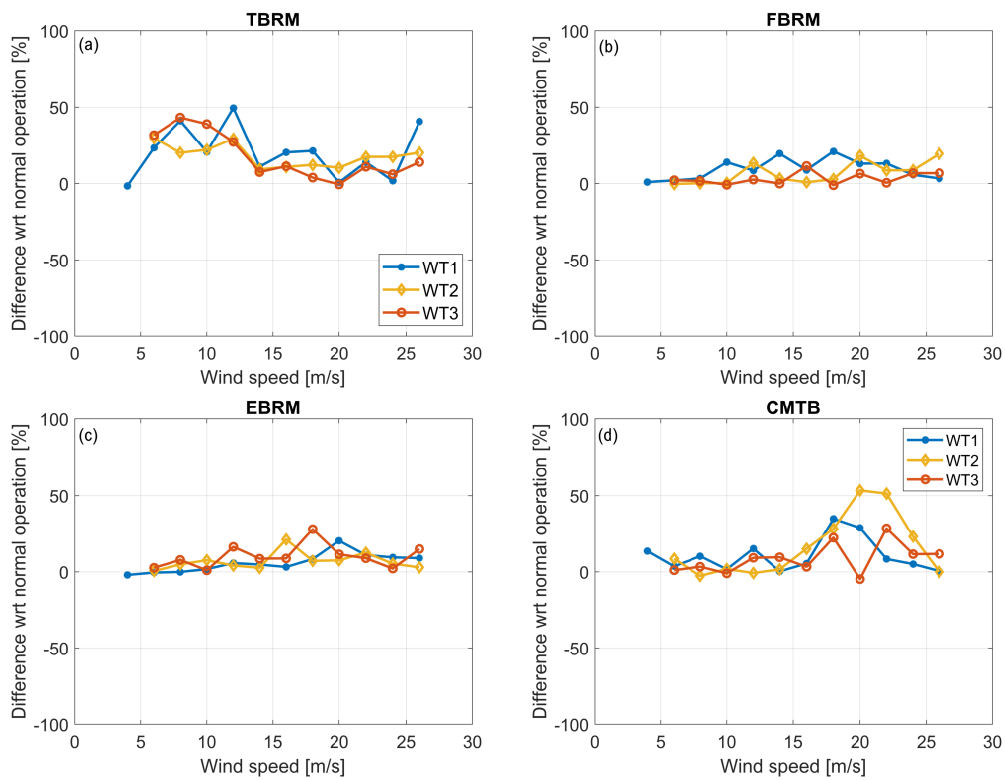
Figure 8: Relative difference between the maximum value of operation under extreme yaw misalignment with respect to the maximum value of operation under normal yaw misalignment, as defined inSection 4.2.2, for selected load sensors. The relative difference is computed for each wind speed and each reference model.
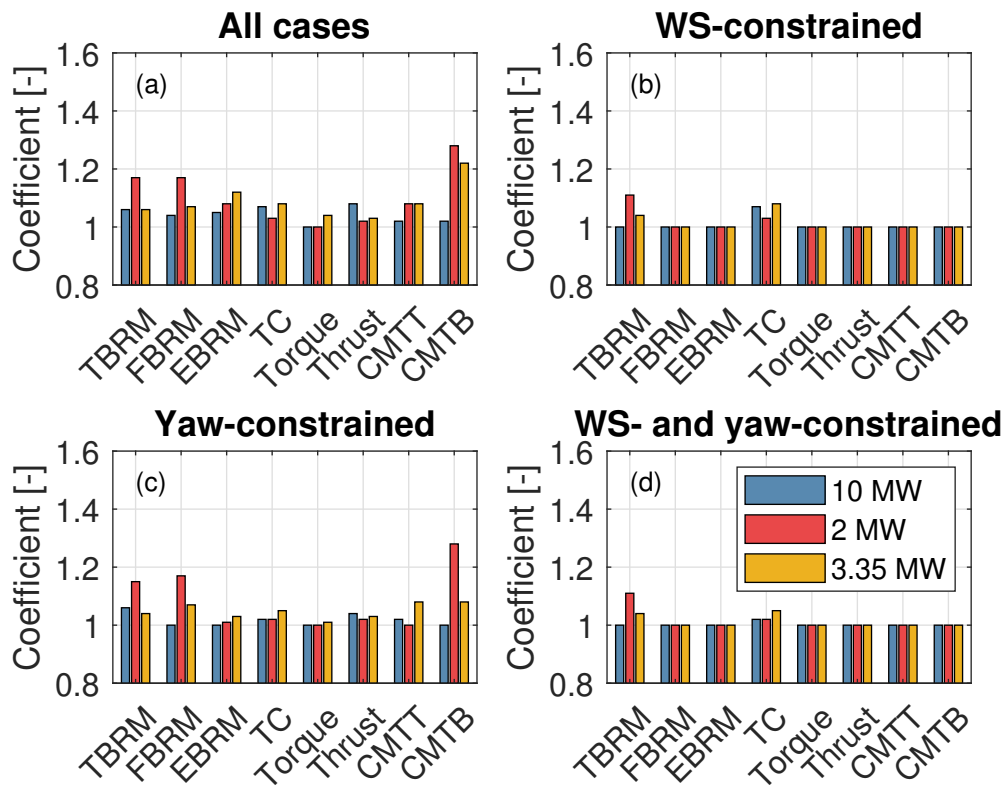
Figure 9: Comparison between the safety coefficients obtained with *Cp-Lambda*
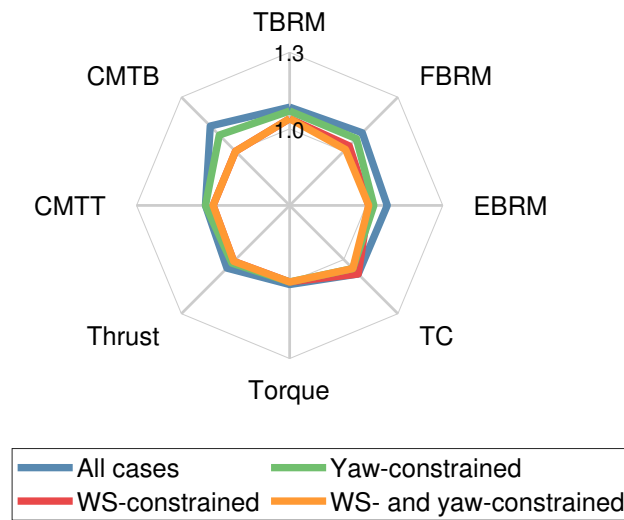for three reference models, and the four scenarios considered (see text).

Figure 10: Average safety coefficient, considering all the reference models considered in this study.

4.4   Summary

This study has analysed the impact of yaw misaligned operation in the extreme loads of three reference models. The study has focused on extreme loads occurring during power production conditions (DLC1.X) and considers a range of yaw misalignments from -38° to +38°, and wind speeds from cut-in to cut-out. Simulations are run for multiple seeds, two aero-servo-elastic simulators and three different reference models. The following trends are identified in the studies presented here:

- From the design load cases considered, DLC1.3 is identified as the design load case driving the maximum values under extreme yawed operation

- Flapwise and edgewise bending root moment increase after rated wind speed for operation in extreme yaw misalignment.

- Tower clearance also presents a lower value after rated wind speed, implying an increase of blade tip deflection.

- The combined moment at tower bottom increases significantly after rated wind speed.

These trends are quantified through safety factors, which are here defined for each quantity of interest as the ratio between the maximum value of this load sensor for operation in normal yaw misalignment ($\pm 8°$, $0°$), and the maximum value for operation in extreme yaw misalignment ($\pm 38°$, $\pm 30°$, $\pm 25°$, $\pm 20°$, $\pm 15°$ and $\pm 10°$). Based on the trends identified, four scenarios with different wind speeds and yaw misalignments are considered. Figure 10 presents the average safety factor (computed with the safety factors of all machines here analyzed) for each of the four scenarios. Results show that the tower is the component that receives the highest impact, as visualised by the large safety factor in the scenario without restrictions – indicated with "all cases". This safety factor, however, decreases when restricting the range of yaw misalignment conditions, for both wind speeds and yaw misalignment. The safety factors relative to blade quantities (TBRM, FBRM, EBRM) also decrease when increasing the restrictiveness of operation in yaw misalignment. Tower clearance (TC) shows here a value higher than 1 for all the four scenarios analysed. It should be here remarked that this does not imply the same impact in tip deflection and therefore, the implication of this higher safety factor in the blade design should be carefully analysed.

Overall the results of this study – even if still preliminary trends – show that operation in extreme yawed conditions do not necessarily lead to higher extreme loads, if the operating range (yaw misalignment and wind speed) is carefully chosen. Clearly, further work should be performed to validate and refine the trends here identified. For instance, further studies should investigate how the logic of the yaw controller can impact the extreme loads, as well as include more reference models. Additionally, other operating cases beyond DLC1.X should also be analysed, and fatigue loads should be included.

5   WFC load prediction with state-of-the-art tools

In the previous section 4 the impact of the WFC strategy "wake steering" on the ULS loads of individual turbines has been demonstrated. Within this section simulation tools under development are introduced which allow to generate a complex loading picture not just of one single wind turbine but on all wind turbines within a large wind farm. Here the focus is on the distribution of Fatigue Limit State (FLS) loads across the wind farm. The FLS loads are typically expressed by Damage Equivalent Loads (DEL) for the full operational life time of the wind farm. DEL's are based on the Palmgren-Miner rule which assumes a linear damage accumulation of all load cycles experienced during the operational life time and are related to a predefined load cycle reference number [27].

A key element for the numerical description of flow conditions within a wind farm is the realistic modelling of the physics of the wake effects. Wakes are energetic circulating vortexes behind the rotor plane of an operating wind turbine tripping downstream. The disturbance of the inflow of the downstream wind turbines causes additional damage to the wind turbine components. Therefore, this section provides a detailed insight into the difficulties of numerical modelling of complex wake situations but also into solutions using simplified approaches to compute the flow flied in a wind farm in reasonable accuracy and computation time.

In the early wind standards the wake effects have been expressed by an increase of turbulence intensity depending on the S/N curve slope of the corresponding loaded component, see Frandsen approach in IEC61400-1:2005 Edition 3.0. This simplified approach has been replaced by the Dynamic Wake Meandering (DWM) method in order to capture dynamic wake effects and has been affiliated in IEC61400-1:2019 Edition 4.0 [1]. Both methods are capable of handling de-rating strategies such as axial induction. However, none of them contains a sufficient description of wake effects under operation with large yaw misalignment angles.

Further information on the historic development of wake models and the state-of-the-art of wake modelling are given in FarmConners deliverable D2.1 [35] and in TotalControl deliverable D4.7 [30].

5.1   Overview on wind farm simulation tools

Currently, many attempts are made to extend the DWM method and to model the wake effects also for wake steering conditions. The following compilation of recent simulation tools have been considered during FarmConners research work. The following compilation does not claim to be complete since there are many more sophisticated wake modelling codes in development.

One group of tools could be categorised as low-fidelity wake models, based on integral relations of fluid mechanics, where the rates of change of fluid momentum and mass must be conserved across a specified control volume, like the *Park wake model* [46], [33]. The possibility to combine these models with effects of yaw misalignment analytically was done in [32]. A simple formula was proposed to predict the wake skew angle based on the momentum conservation and top-hat model of [46]. Using this approach, a formula for the yaw induced wake centre trajectory was derived by integrating this skew angle [31] and implemented in *FLORIS* model (FLOw Redirection and Induction in Steady-state).
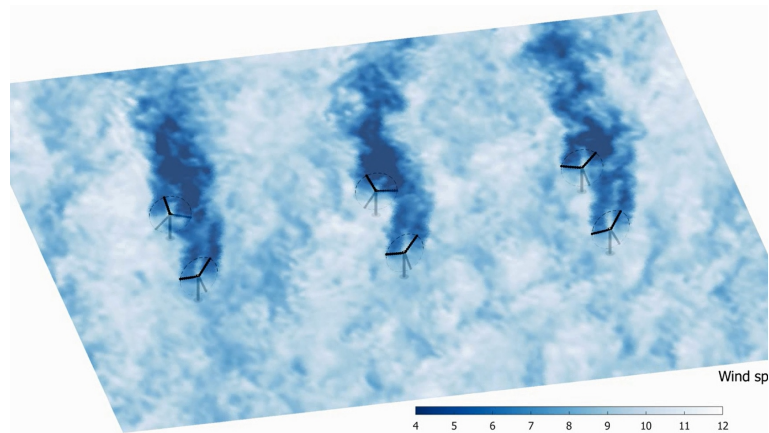
Figure 11: *FLORIS* simulation - TU Delft, B.M. Doekemeijer et al.

A medium-fidelity DWM model is implemented in NREL's software *FAST.Farm* [39]. By simple extensions to the passive tracer solution for transverse wake meandering, the wake-dynamics solution in *FAST.Farm* is extended to account for wake deflection and wake advection. The passive tracer solution enables the wake centreline to deflect based on the inflow skew, since in this case the wake deficit normal to the disk introduces a velocity component that is not parallel to the ambient flow. In addition, *FAST.Farm* uses atmospheric phenomena generated by a precursor LES simulation of the entire wind farm.

Other examples of medium-fidelity wake models are *WFSim* [54] or *FarmFlow* (*WakeFarm*) [2], which solves a two-dimensional form of the unsteady turbulent Navier-Stokes equations along a horizontal plane located at the hub height of the wind turbines within a wind farm, which simulates the wind turbine wakes by solving the steady parabolised Navier-Stokes equations in perturbation form in three dimensions.

The high-fidelity tools with wake models, relying upon differential relations of fluid mechanics. High-fidelity wind farm models generally employ large-eddy simulations (LES), which solve temporally and spatially-filtered forms of the three-dimensional Navier-Stokes equations that only capture eddies of relevant scale. One example of a high-fidelity simulation tool that is commonly used for wind farm controller evaluation is *SOWFA* (Simulator fOr Wind Farm Applications), developed by NREL [45].

Another widely used tool is *EllipSys3D*, developed by DTU [50] and [47]. About their applicability in the context of wake steering, see e.g. [51] and [52].

Other three-dimensional LES-based simulators developed specifically for wind farm applications include *SP-Wind*, developed by KUL [44], are *UTD Wind Farm* [43] or *PALM* (Parallelized LES Model) [5]. They reduce the computational cost of simulations by modelling wind turbines using actuator disc theory.

A new approach of implementing the DWM method is a combination with so-called surrogate models. This approach can speed up the load estimation at different positions within the wind farm remarkably and therefore can play a crucial role for wind farm optimisation purposes. One of the simulation tools that has implemented and extended this approach is *LongSim*. This tool is introduced in more detail in the following section.

5.2   WFC simulation code LongSim

LongSim is a wind farm modelling software code developed by DNV, with the primary function of designing, testing, evaluating and certifying wind farm controllers.The code is still in development stage and not commercially available

yet.

A primary requirement is to be able to run rapid calculations of wind farm wake effects, both in the steady state and in realistic dynamic conditions. To achieve the required calculation speeds and low computational requirements, the wakes are represented by engineering models embedded an underlying flow field, without the use of computational fluid dynamics (CFD). Also, the wind turbines are represented without detailed blade aerodynamics or structural dynamics, although the controller operation can be modelled in detail, including supervisory and yaw control. However, since turbine loading considerations can be important, the loads are represented using a surrogate model derived from targeted simulations using a detailed single-turbine aero-servo-elastic model, in this case the time domaine simulation code *Bladed* [15].

A brief general description of *LongSim* is provided in Section 5.2.1 and Section 5.2.2, followed by the description of the surrogate loads modelling. Some application examples and code-to-code comparisons are presented in Section 5.2.3.

5.2.1 General principles

Wakes in *Longsim* are modelled by means a Gaussian velocity deficit profile behind each turbine which becomes broader and shallower as it dissipates downstream. A number of such models are described in the literature, see Section 5.1, and *LongSim* includes many different variations: not only for the characterisation of the Gaussian shape, but also for the additional turbulence in the wake, the deflection of the wake centreline due to turbine yaw misalignment, and the way in which multiple wakes combine at points inside the wind farm. Recent usage has tended towards a particular combination of model features which appear to work well across a wide range of wind farm data sets used for an ongoing validation programme.

For dynamic simulations, the wakes are embedded in a stochastic wind field with realistic spatial and temporal coherence properties. The wind field can follow measured low-frequency wind variations, for example from a met mast, to give a realistic representation of changing meteorological conditions over many hours or days. Low-frequency wind field variations cause the turbine wakes to meander, and together with high-frequency turbulence at each turbine, cause changes in the turbine operation defined by the turbine aerodynamics and control logic. The resulting changes in the wake properties then advect downstream.

The turbines themselves can be modelled either using power and thrust look-up tables, or in a more detailed representation using rotor power and thrust coefficients to represent the aerodynamics, in combination with the turbine pitch-torque control and the rotor speed, pitch and yaw degrees of freedom. Supervisory control features can be modelled in a very flexible way, including a detailed representation of the yaw control logic for example.

Depending on the level of detail required for the control, the simulation timesteps are typically of the order of 0.1 to 10 seconds, with longer timesteps resulting in faster simulations. The combination of a relatively long simulation timestep with long-term wind field variations mentioned above is very appropriate for wind farm control investigations. However, to predict turbine loads it is necessary to have a full aeroelastic model of the turbine driven by a non-uniform, turbulent flow through the rotor, for which much shorter timesteps would be needed, of the order of 20 − 50 ms. For this reason, a surrogate model based on the aeroelastic code *Bladed* has been developed. The model, which is fitted to a detailed set of *Bladed* aeroelastic simulation results for any target turbine, is incorporated in *LongSim*, allowing it to give a suitably detailed representation of the turbine loading with almost no compromise in run time. This model is described in the next section.

5.2.2 Surrogate loads model

LongSim now includes two different surrogate models based on *Bladed* aeroelastic simulation results. The original model interpolates loads from a Fatigue Loads Database (FLD) consisting of Damage Equivalent Loads (DEL's) calculated from a large number of 10-minute *Bladed* aeroelastic simulations, arranged in a multi-dimensional look-up table. Each dimension, or axis, represents one of the input variables defining the simulation wind conditions. As a minimum, the axes should include:

- Wind speed

- Turbulence intensity

- Wind shear

With a sufficient number of points N_i along each axis i. This requires ΠN_i simulations, which is quite tractable for a small number of dimensions. However, other factors which affect the loads may be important, depending on the application, for example veer and air density, and for wind farm control applications there would be yaw misalignment for wake steering and thrust reduction settings for axial induction control. Wake effects within a wind farm can be represented by the increased turbulence intensity, but this ignores the additional loading effects of partial wake immersion, and wake meandering always plays a role. With too many axes, the number of simulations required to populate the hyper cube of different conditions rapidly becomes prohibitive.

For this reason, a new surrogate model has been developed which circumvents the "curse of dimensionality" by attempting to separate the different effects, modelling each effect in isolation from other effects, and then combining the different contributions.

An overview of the model structure is illustrated in Figure 12. The green boxes on the left describe the physical inputs which are assumed to have an effect on the loading. Next, the blue boxes describe the way in which the effect of each input on the loads is modelled, to represent the load in the manner described in the purple boxes. The grey boxes show how the loads are transformed into the time domain, where the various components are summed.

The various loads which are so far included in the *LongSim* model are listed in Table 5, using the *Bladed* coordinate system (right-hand axes with x aligned to the nacelle direction and z vertical, tilted through the shaft tilt angle in the case of hub loads). It is very straightforward to add more loads as required. The "Sum of blade root My" is as a fixed frame load representing the sum of the blade root out of plane moments over all the blades, and is used in constructing the individual blade root out of plane moments in the rotating frame.

The turbulent stochastic load components shown in Figure 12 represent variations around the mean. The deterministic components are mostly at blade passing frequency (3P, assuming three blades), and so are also zero-mean, but in some cases there are 0P components which provide a non-zero mean value, in particular for the nodding and yawing moments, which have a non-zero offset due to asymmetries in the flow field from the various deterministic causes. For the other loads, the non-zero offset is determined using "DC gains". The sources of the non-zero offsets are shown in Table 5. The DC gains represent the ratio of each load to either the thrust or torque. Some of these ratios are straightforward, as shown in third column of Table 5, otherwise they are obtained simply from a *Bladed* steady loads calculation, as a function of wind speed. *LongSim* applies these multipliers to the (time-varying) rotor aerodynamic torque or thrust which it already calculates from the turbine properties and the wind conditions.
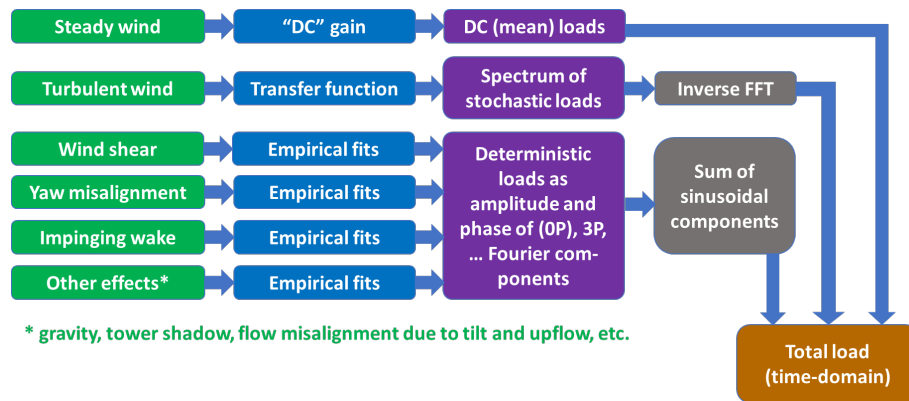
Figure 12: LongSim-Structure of the model

Table 5: LongSim load components

Load component	Frame	Source of DC component
Hub Fx (thrust force)	Fixed	DC gain from rotor thrust, plus 0P for "other effects" only
Hub Mx (torque)	Fixed	DC gain from rotor torque
Hub My (nodding moment)	Fixed	0P deterministic
Hub Mz (yawing moment)	Fixed	0P deterministic
Tower base Mx	Fixed	DC gain from rotor torque
Tower base My	Fixed	DC gain from rotor thrust, plus 0P for "other effects" only
Sum of blade root My	Fixed	DC gain from rotor thrust
Yaw bearing Mx	Fixed	DC gain from rotor torque: cos(tilt)
Yaw bearing My (nodding moment)	Fixed	0P deterministic
Yaw bearing Mz (yawing moment)	Fixed	DC gain from rotor torque: -sin(tilt), plus 0P deterministic
Blade root Mx (in-plane moment)	Rotating	DC gain from rotor torque: 1 / no. of blades
Shaft My (bending moment)	Rotating	Derived from other loads
Blade root My (out of plane moment)	Rotating	Derived from other loads

Note that the *Bladed* steady loads calculation does not include the "other effects" (mainly gravity), so it is necessary to include this deterministic 0P component in the case of the Hub Fx and Tower My; the other 0P deterministic effects would come through anyway via the DC gain, and must not be double-counted. Apart from the 0P components in Table 5, the deterministic effects are all represented by the 3P Fourier component for the fixed-frame loads, and the 1P component for the blade root Mx which is in the rotating frame. It is very straightforward to extend this to other harmonics if necessary – for example the fixed-frame 6P and 9P components might be important for some turbines. The blade root out of plane and shaft bending moments are derived directly from the other loads, so their own DC, stochastic and deterministic components to not need to be modelled separately. Thus, the blade root out of plane bending moment for blade i is calculated from the hub nodding and yawing moments M_y and M_z by means of the Coleman transformation:

$$M_{bri} = (\frac{2}{N_B}) \left(M_y cos(\Theta + \frac{2\pi(i-1)}{N_B}) + M_z sin(\Theta + \frac{2\pi(i-1)}{N_B}) \right) + \sum \frac{M_{br}}{N_B} \qquad (1)$$

where N_B is the number of blades, Θ is the rotor azimuth angle, and the offset $\sum M_{br}$ is the sum of the blade root bending moments over all the blades, which has been modelled along with all the other fixed-frame loads as described above. The resultant shaft bending moment is given by $\sqrt{M_{ys}^2 + M_{zs}^2}$ where the individual rotating components are obtained by rotational transformation:

$$M_{ys} = M_y cos(\Theta) + M_z sin(\Theta) \qquad (2)$$

$$M_{zs} = M_z cos(\Theta) + M_y sin(\Theta) \qquad (3)$$

Deterministic components

Deterministic effects represent the effect of steady non-turbulent asymmetries affecting the loads. These effects are different on each blade, in a way that depends only on the azimuthal position of the blade. So far, the following effects have been considered:

- Wind shear

- Yaw misalignment

- Gaussian wake of an upstream turbine

- Tower shadow

- Flow misalignment due to rotor tilt and upflow

- Gravity

The first three effects can vary, whereas the last three can usually be considered unchanging.

It would be straightforward to extend the model to include other deterministic effects, for instance wind veer, rotor imbalance, etc.

As the influence of these effects on loads depends on rotor azimuth, Fourier decomposition can be used to calculate the amplitude and phase of each rotational harmonic contributing to the load variations. Symmetry dictates that only multiples of the blade passing frequency can have an effect on fixed-frame loads, so for a three-bladed turbine, only the Fourier harmonics at 0P, 3P, 6P etc. are relevant. In the rotating frame, all harmonics (0P, 1P, 2P …) can potentially contribute.

The three unchanging variables can be treated together, so at each wind speed, just one simulation is needed where all the three effects are present, compared to the same simulation where they are all switched off (note that flow misalignment due to rotor tilt and upflow is switched off by setting the upflow to the negative of the rotor tilt). At each simulated wind speed, the Fourier harmonics for each load are calculated in a post-processing step. For intermediate wind speeds, *LongSim* linearly interpolates the amplitudes and phases of the Fourier harmonics. This is more straightforward if they are first converted into the equivalent orthogonal (y and z) components. These simulations are run with constant uniform zero-turbulence wind input, with no asymmetries other than those for which Fourier harmonics are to be calculated. The simulations can therefore be fairly short – just long enough for any transients due to imperfect initial conditions to die away, and then a few further rotor rotations from which the Fourier harmonics are calculated.

The first three effects in the list above can vary independently, so they must be treated individually, and Fourier harmonics calculated for different values of the input parameters defining the asymmetry: different wind shear exponents,

29

different yaw misalignments, and different parameters defining the velocity deficits in a Gaussian wake. The required simulations are again short, with uniform steady wind and no asymmetries apart from the particular effect being char-acterised. The Fourier harmonics will vary according to the input parameters defining the asymmetry, so for each case an empirical model is fitted to the results, to give the y and z components of each Fourier harmonic as a function of the input parameters.

A set of base case simulations has also run, with no deterministic inputs. The base case Fourier amplitudes should be zero for these runs; nevertheless, the Fourier amplitudes for each deterministic effect are adjusted by subtracting the corresponding base case Fourier amplitude, just in case they are not exactly zero for whatever reason.

The empirical fits are based on simple polynomials. A 3rd-order polynomial on wind shear exponent works well. For yawed loads, 4th-order polynomials on yaw misalignment fitted separately for the positive and negative yaw directions work reasonably well.

Wake effects are more complicated as they depend on three input parameters: the centreline deficit δ, the wake width ω, and the wake centreline displacement at the downstream turbine (displacements in the y and z directions are equivalent by rotational symmetry, so the phase of each Fourier harmonic is simply adjusted by the 'phase' of the displacement direction). Using an explanatory variable

$$\zeta = exp\left(-0.5(\frac{y+R}{\omega})^2\right) - exp\left(-0.5(\frac{y-R}{\omega})^2\right) \tag{4}$$

to represent approximately the wind speed change across the rotor of radius R, polynomial functions of ζ and δ or their product were found to fit satisfactorily, although better formulations can be envisaged.

Stochastic components

The stochastic components are modelled by transfer functions from wind speed longitudinal component to each load. *LongSim* then generates loads by multiplying the transfer function by the turbulence spectrum, and using an inverse Fast Fourier Transform to generate time-domain loads (using the same random phases as used to generate the wind speed time histories). Adding transfer functions from the lateral component is also helpful for some loads, notably the tower side-side moments. The vertical component could easily be added in the same way if desired. The transfer functions are generated by post-processing results of 10-minute *Bladed* simulations with turbulent wind, but with all the deterministic effects switched off. Only one simulation per wind speed is needed: turbulence intensity is accounted for in *LongSim* simply by scaling the resulting stochastic loads by the wind speed standard deviation. This works because the transfer functions are effectively independent of turbulence intensity, as illustrated in the example of Figure 13 (the transfer function magnitudes have been filtered using a median filter with a variable order which increases towards the higher frequencies).
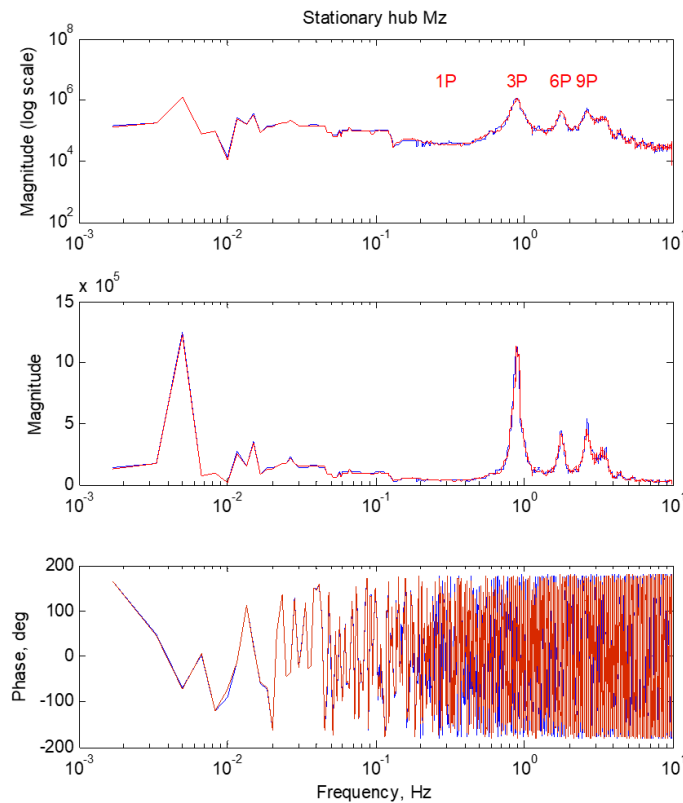
Figure 13: Example transfer functions at 9 m/s: 10% TI (blue), 20% TI (red)

5.2.3   Verification against Bladed

The model's key assumption is that the load components described above can be calculated separately and then added together. To test whether this assumption is reasonable, a *LongSim* simulation setup with two turbines has been devised which allows the predicted loads to be compared directly against the results from a full aeroelastic simulation using *Bladed*. The setup is illustrated in Figuree 14, and represents turbines A-07 (upwind) and A-06 (downwind) at Lillgrund wind farm, which are separated by 400 m and aligned in the 222º direction. The wind field is a uniform 8.8 m/s with 10% ambient turbulence, from which high-frequency wind speed variations at the two turbines are generated using a Kaimal spectrum. The wind direction is 214º, resulting in a 48.8m lateral offset of the wake of the upstream turbine at the downstream one (approximately half the rotor diameter). The wind shear exponent is 0.14, and the downstream turbine is yawed at 22º to the wind direction. All these values are deliberately chosen not to match values for which the model is fitted, so that the interpolation of model parameters is included in the testing. For each turbine individually, the same conditions can be set up in *Bladed*. For the downstream turbine, the 'upwind turbine wake' feature in *Bladed* allows the Gaussian wake of the upstream turbine to be defined. For comparing to *Bladed*, a uniform wind field was used in *LongSim* so that there is no underlying low-frequency variation, and hence no wake meandering. A snapshot of the setup is shown in Figure 14. A second test with the second turbine unyawed was also run.
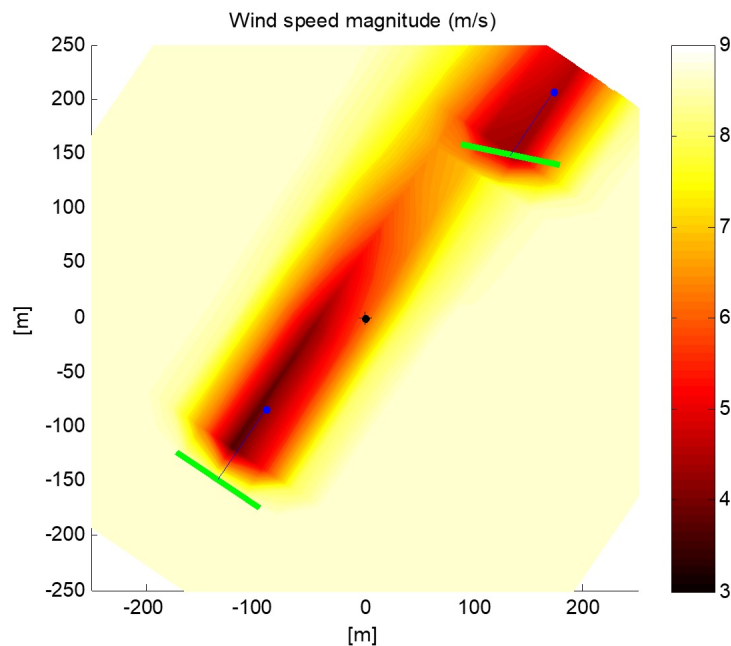
Figure 14: *LongSim* run for comparison against *Bladed*: snapshot of wind speed contours

Although the mean conditions at each turbine can be matched between the two codes, including the wind shear and wake, it is not possible for the complete stochastic wind conditions to be matched. *Bladed* models the stochastic variations over the whole rotor, while *LongSim* only models the wind speed at the hub, with the effect of turbulent variations across the rotor coming from the stochastic transfer functions. Therefore, the loads will not match exactly in the time domain, especially at the higher frequencies, but the resulting spectra of the loads should be similar. Damage equivalent loads (DEL's) should also be similar, although the random turbulence seed can have a big effect on some loads, so three different seeds have been run for each simulation to indicate the spread in the DEL's.

Examples for a couple of key load sensors are shown in Figure 15 and Figure 16. Results are shown in three columns: the upstream turbine, the downstream turbine unyawed, and the downstream turbine in the yawed case. The spectra show very good agreement. There are differences in some of the DEL's between *LongSim* and *Bladed*, but they are typically no greater than the differences arising from the different random number seeds. A few seemingly more systematic differences were found: for example, for this particular turbine, the Hub Mz DEL's of the downstream turbine seemed to be about 20% higher then in *Bladed*, but by running more seeds and modifying the filtering of the low-frequency end of the transfer functions, which are very seed-dependent, the discrepancy was reduced. In general, the comparison does support the assumption that adding the different deterministic and stochastic load contributions in the time domain is a reasonable approach.
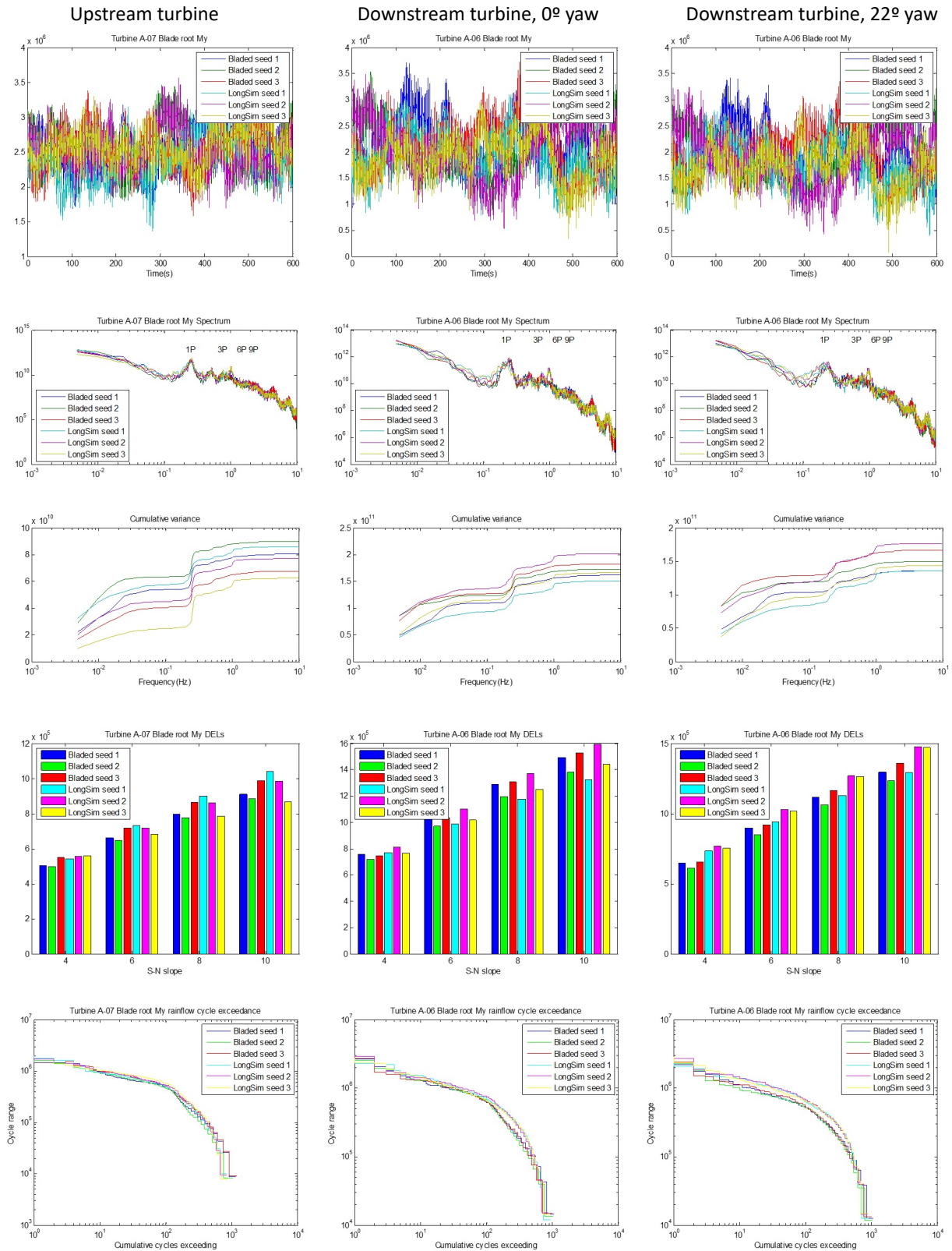
Figure 15: Blade root My. From top to bottom: Time histories, spectra, cumulative variance, damage equivalent load, rainflow cycle exceedances
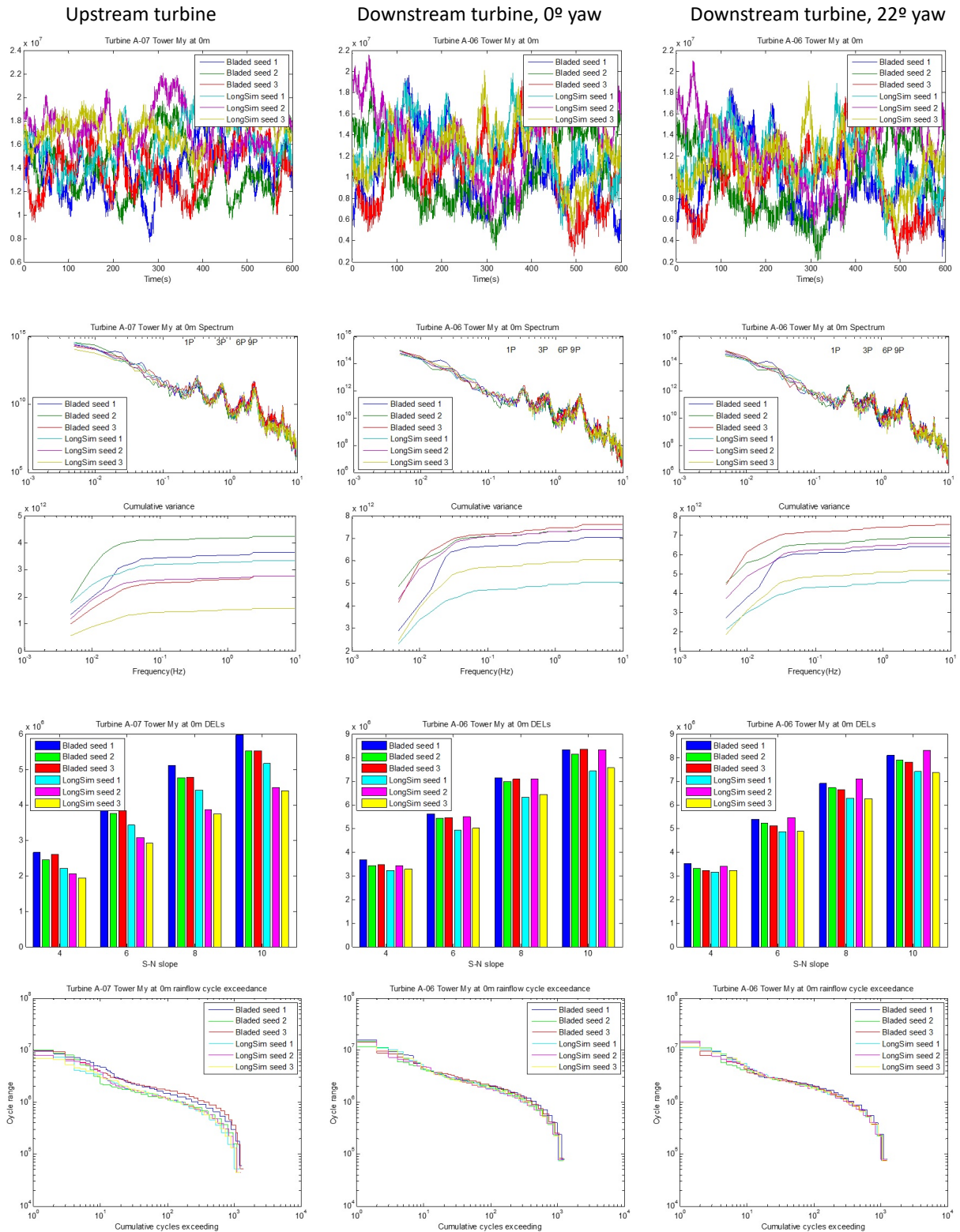
Figure 16: Tower base My. From top to bottom: Time histories, spectra, cumulative variance, damage equivalent load, rainflow cycle exceedances

5.2.4   Summary

This modelling framework offers the potential to take account of turbine loading when optimising setpoints for wind farm control, and also for loads to be output from time-domain simulations: as time-series of 10-minute damage equivalent loads, as well as actual high-frequency (e.g. 20Hz) load time histories, for any or all turbines in the wind farm. This is achieved without significantly slowing down the simulations: the illustrated 22-hour simulation for a 48-turbine wind farm ran in about 15 hours on a standard laptop computer.

To generate the loads model in the first place requires a rather small number of *Bladed* simulations: for each, a few hundred steady wind simulations of 100 seconds length, and just eight 10-minute turbulent wind simulations, were needed. With five induction control setpoints, these runs easily ran overnight on a standard laptop computer. The empirical fitting to create the loads model from the simulation results takes a similar time.

Comparison against *Bladed* simulations suggests that the key assumption, that the different loading contributions can be calculated independently and combined in the time domain, is reasonable.

5.3   Exemplary FLS anaylsis of Lillgrund offshore wind farm

LongSim can use the surrogate loads model both for steady-state calculations, including setpoint optimisation for wind farm control, and in dynamic simulations. For steady-state calculations, 10-minute load time histories are generated for the mean conditions at each turbine, using the appropriate turbulence intensity for stochastic loads combined with the required deterministic effects, and used to calculate the 10-minute DEL's. These DEL's can also be included in the merit function against which wind farm control setpoints are optimised: different weightings can be applied to the power output and any key loading metrics, for example the mean and maximum tower base and blade root DEL's across all the turbines.

An example is shown in Figure 18, which shows the result of setpoint optimisations for the 48-turbine Lillgrund offshore wind farm, for one specific wind condition (9 m/s, 6% turbulence intensity and wind direction 222º blowing directly along the principal rows). The different colours show total wind farm power, and the highest turbine blade root and tower base DEL's (with appropriate Wöhler exponents) across the whole farm. The different cases are induction control (IC), wake steering (WS) and both combined, when optimised either for total power or for a weighted combination of power and loads (as indicated in brackets).
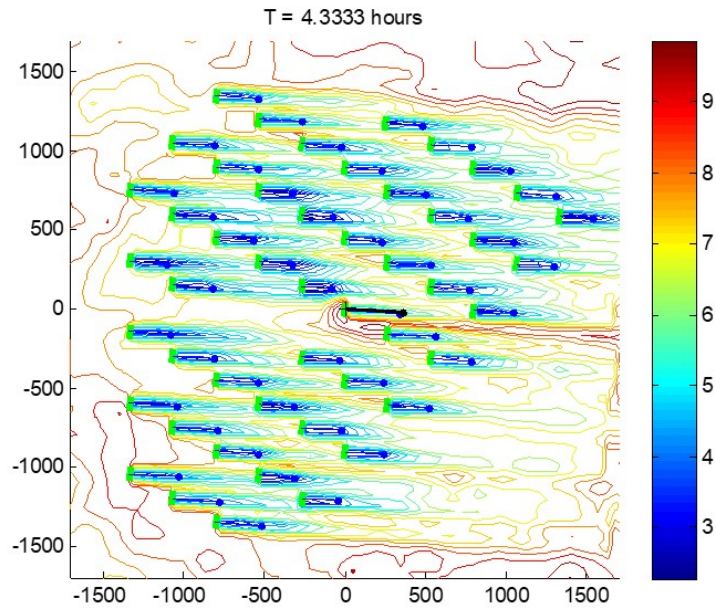
Figure 17: LongSim dynamic simulations of Lillgrund offshore wind farm with 48 turbines of 2.3MW

Beside the predicted power yield two load sensors, namely blade root flapwise bending moment and tower bottom fore-aft bending moment, have been selected to demonstrate the impact of WFFC strategies of FLS loads and DEL's respectively.
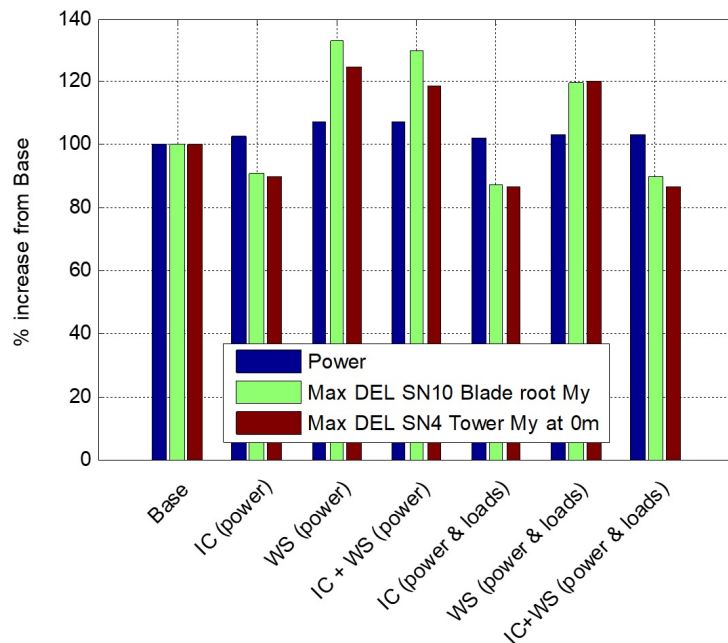

Figure 18: Comparison of induction control and wake steering optimisations, including load effects

This example shows that for this wind condition, induction control increases the power output by about 3% while the

maximum loads decrease by about 10%. Wake steering achieves a higher power gain (7%) but the loads are also significantly increased. Combining induction control with wake steering yields very slightly more power than wake steering alone, and the loads do not increase quite as much. By including the loads in the merit function they can be reduced further, with an inevitable compromise on the power gain.

Figure 18 is for a single wind condition; for a full assessment this would be repeated for the full range of wind conditions expected at the site, and each result weighted according to the probability of occurrence of the particular wind condition.

This example illustrate that further validation is required however, and especially important is the need to validate results against turbine loads measured in the field in multiple wake conditions inside a wind farm [36] .In line with a comprehensive code validation of *LongSim*, the tool could be applied in future certification processes, e.g. to identify the highest loaded wind turbine or the maximum loaded components within a wind farm which is operating with a specific WFC concept. The critical location(s) with respect to FLS loading could be selected and further analysed in more detail taking the flow conditions determined by *LongSim* into consideration. This detailed analysis of the identified locations could be performed with existing state-of-the-art aero-servo-elastic simulation tools such as *Bladed*, *HAWK2*, *FAST*, *Flex5*, etc. to verify structural integrity under WFC operation.

6 Experimental benchmark tests with WFC operation in the field

6.1 Practical implementation of WFC

In the past few years, ENGIE Green has conducted several wind farm control field tests in one of its wind farm, as part of the French national project SMARTEOLE. Those experiments were focused on both axial induction and wake steering control and built on each other: while the first field tests were rather simply implemented, the final ones were designed with great care in order to assess the benefits and load impacts of the WFC strategy.

This section offers a quick summary of main outcomes that could be derived from these experiments in terms of both power and loading for the wind turbines considered during the field tests. Figure 19 represents the timeline of SMARTEOLE project while a more detailed description of each field test can be found in Table 6. Comprehensive analysis of the results obtained were published in [3, 24] for field campaign #1, [37, 25, 57] for field campaign #2, and [56] for field campaign #3.

Figure 19: Timeline of SMARTEOLE field test campaigns.

Field tests	Strategy tested	Date of test	Type of test
#1	Axial induction	from 2015-12-21 to 2016-04-29	Basic curtailment at 1200 or 1600 kW depending on the wind speed, activated manually by the operator when wind conditions were satisfactory.
	Wake steering	from 2016-08-02 to 2016-09-08	Constant misalignment applied on the turbine, first +12° during 10 days and afterwards -8° during 3 weeks.
#2	Wake steering	from 2017-08-12 to 2017-10-03	Constant misalignment applied on the turbine, approximately +13 - 15° during the full duration of the tests.
	Axial induction	from 2017-12-14 to 2018-02-09	Automatic activation of a noise reduced operation mode (NRO), close to optimised axial induction control operation. The NRO mode was toggled on and off every hour during the night.
#3	Wake steering	from 2019-12-18 to 2020-08-07	Optimised wake steering control applied through a control box, designed specifically for the field tests to misalign conveniently the turbine. The wake steering control was toggled on and off every hour.

Table 6: Description of the three field test campaigns of the SMARTEOLE project.

6.1.1 Experimental setup

The SMARTEOLE field tests were all realised on the wind farm *Sole du Moulin Vieux (SMV)*, whose layout is represented on Figure 20. It consists of 7x Senvion MM82 2.05 MW wind turbines oriented in a more or less linear layout, from North to South. The experiments were led on two turbines of the farm, SMV6 and SMV5, due to the short distance between and their alignment close to the direction of the prevailing winds at the site. An extensive instrumentation was deployed for all field campaigns, as displayed on the figure. Furthermore, strain gauges were also installed on the turbine blades allowing to measure the changes in loading due to the application of WFC during field tests #2.
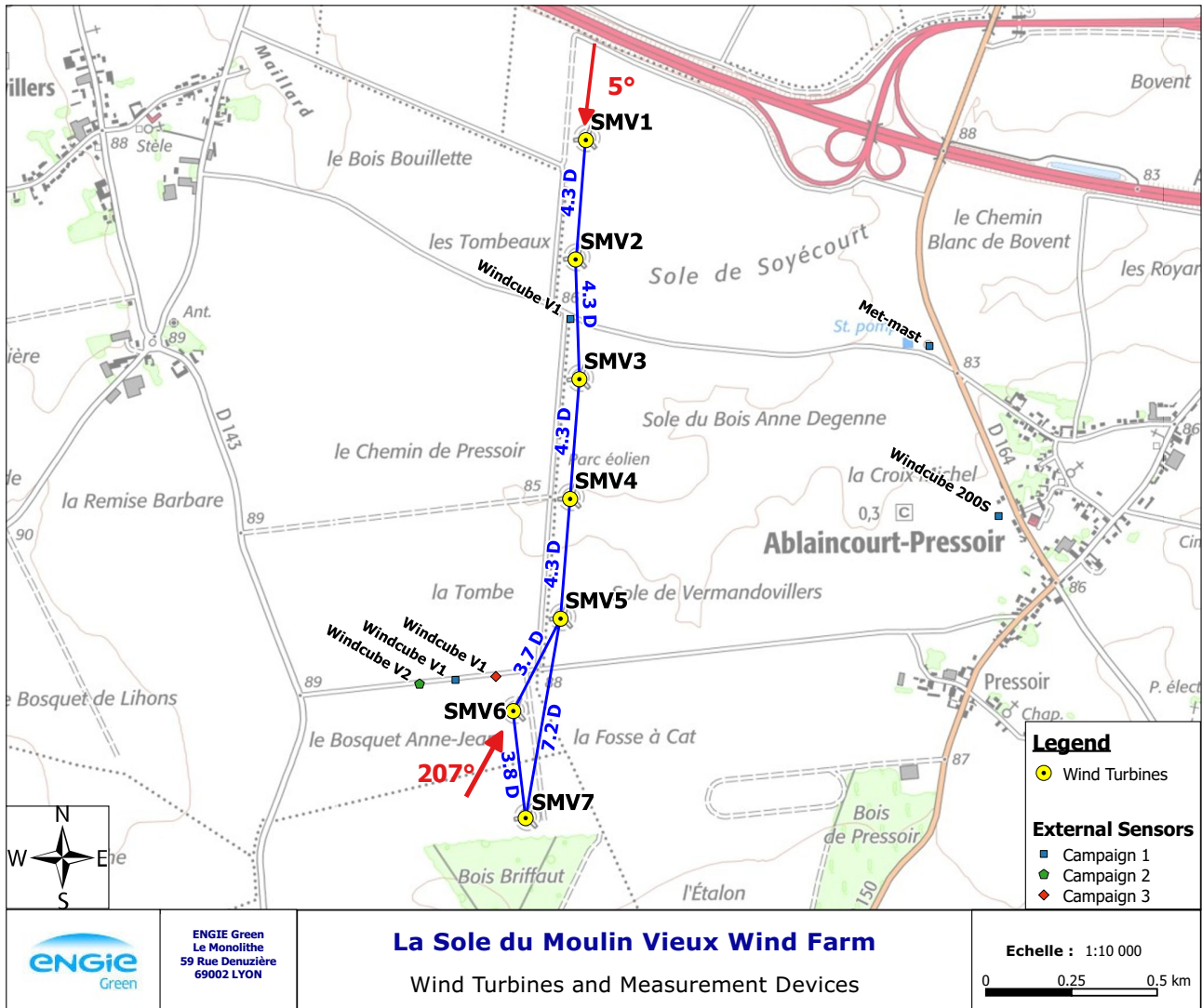
Figure 20: Map of SMV wind farm. Wind turbines in the farm are represented along with inter-distances between them expressed in turbine diameters (with D = 82m) and main wind direction angles. Locations of external sensors installed for each campaign are also indicated.

6.1.2 Impact of WFC on power production

The section recaps the main findings from SMARTEOLE project in terms of power production, for both WFC strategies.

Regarding axial induction control, two experiments were led. In field tests #1 the derating of the upstream turbine was too strong and even though increase in downstream turbine production could be observed, it was not compensating for the upstream loss. A much sophisticated strategy was designed for field tests #2. However due to operational constraints it was not possible to implement the calculated optimal set-points within the turbine ; instead, a predefined noise-reduced operation (NRO) mode was used. According to simplistic wake modelling simulations, this NRO was expected to provide increase in power production between 7 and 9 m/s for the two turbine setup. In practice though, no gain in downstream power production were found, while the upstream turbine was experiencing power losses due to the

derating. Consequently no gain in power production could be achieved through this control strategy, however it was beneficial for load reduction as it will be presented in the next subsection.

Conversely, the wake steering field tests were much more successful. While the limited amount of data recorded during the first field campaign were not enough to conclude about the benefits of the strategy, some power gains were observed for a certain wind direction sector in the second field campaign #2. An optimised wake steering strategy was then designed for the last field campaign #3based on these first results, and is represented on Figure 21. As it can be seen, the maximum yaw misalignment implemented on the turbine is 20 degrees for full wake conditions and decreases linearly with wind direction for partial wake conditions. Further, when wind speed is higher than 10 m/s, the misalignment is reduced gradually until 14 m/s for which no yaw offset is applied. This strategy was specifically designed to avoid significant loading on the upstream turbine. Indeed, as it is shown in Chapter 4 above, the increase in loading can be very high for the controlled turbine for above rated wind speeds.

This limitation of of the wake steering mode at the test campaign to wind speeds between 3 m/s and 14 m/s and yaw misalignment angles between 0° and ±20° is corresponding to the ULS simulation results found in Section 4.
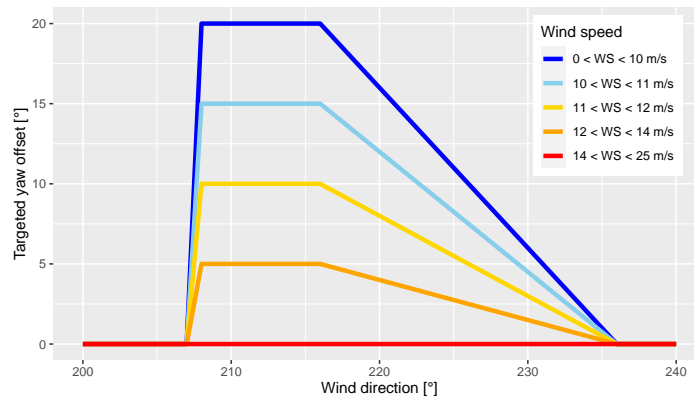

Figure 21: Targeted yaw offsets of the upstream wind turbine as a function of wind direction and wind speed for the final wake steering strategy. Figure taken from [56].

The results from this experiment are thoroughly discussed in [56]. In short, net gains in power production were achieved by this strategy thanks to a reduction of about 5.6% of the wake losses. Interestingly, the power gains were stronger for the near-rated wind speed (from 8 to 12 m/s) than for the lower wind speeds, between 6 and 8 m/s. Indeed, at those higher wind speeds, there were virtually no losses on the upstream turbine due to the misalignment, while the downstream turbine was still benefiting from the decrease in the wake effect. This finding underlines the high potential of wake steering for increasing the energy output of a farm. Also it emphasises the need for understanding better the turbine loading around rated conditions: since higher gains can be obtained at those wind speeds, there could be a temptation for the wind farm operators to follow a greedy approach and apply large yaw misalignment in order to get as much energy as possible. But such a strategy could truly endanger the turbines by increasing dramatically the loading on some of their components.

6.1.3   Impact of WFC on turbine loading

The impact of WFC on turbine loading is now discussed, thanks to the measurements of the strain gauges in the blades during field tests #2. The complete results from this analysis are available in [57].

The study of the loading under an axial induction control strategy showed a very positive impact on the blade loading. Indeed, as the upstream turbine is curtailed, the thrust force exerted on its rotor is reduced and therefore both the absolute and fatigue loads are decreased. In particular, a reduction of 5 to 15% (depending on the wind speed bin) in the Damage Equivalent Loads (DEL's) of the blade root flapwise bending moment were observed on the controlled turbine. In theory, some positive impact could also be expected on the downstream turbine. Indeed, as the wake magnitude emitted by the first turbine is decreased, so does the wake emitted turbulence intensity (TI). This reduction in wake emitted TI could translate into decrease in the fatigue loading at the downwind turbine. However, similarly as for the power production, no impact on turbine loading could be observed on the turbine, probably because because the derating applied was too small. In contrast, during field tests #1 when a much stronger curtailment was set up on the upstream turbine, a decrease in TI at the downstream turbine as measured by the nacelle anemometers [26].

The situation is much more complicated regarding wake steering. As the rotor is being misaligned with respect to the incoming wind, this creates an asymmetry of the loading between the left and the right part of the rotor that could increase the fatigue. In practice though, no augmentation of the blade root DEL's were observed during the wake steering experiments of field tests #2, instead reduction up to 15 to 20% depending on the wind speed were observed. This could be related to the direction in which the rotor is misaligned: by yawing the turbine counter-clock wise (CCW, as it was applied for SMARTEOLE), the angle of attack variation over the blade rotation cycle is reduced which in turns decreases the fatigue. Opposite trends would be expected if the turbine were to be expected by yawing the turbine in the clock-wise (CW) direction, as underlined in the literature [42, 41]. However, even though positive impact on the blade loading can be obtained thanks to wake steering by yawing the turbine CCW, this is not the case for other components such as the tower or the speed shaft. Such loads could unfortunately not be measured in the scope of SMARTEOLE field tests, but other field experiments indicate that increase in DEL's would be achieved for these components [14].

The impact of wake steering on the loading at the downstream turbine is the results of the combination of several effects with opposite trends, as explained in [41]: increase in the wind speed downstream (increases DEL's), reduction of the wake-added TI downstream (decreases DEL's), and modification of the wake trajectory (can decrease or increase DEL's depending on the situation). The latter is more difficult to analyse: as the wake is steered from full wake to half wake operation at the downstream turbine, increase in fatigue loading will be expected, but this augmentation will be compensated by situations in which the wake will be steered from half wake to no wake operation. As a consequence, very limited impact on the turbine fatigue loading would be expected at worst due to the WFC. This is exactly what was observed in the scope of SMARTEOLE field tests: no clear increase or decrease in the blade root DEL could be measured when comparing the wake steering with the normal operation.

6.1.4 Summary

In conclusion, the SMARTEOLE field tests gives some first insights about the impact on turbine loading due to wake steering:

- Axial induction control seems to be very beneficial in terms of load reductions both for the upstream and the downstream turbine.

- The situation is not as clear for wake steering, for which positive or negative trends could be observed depending on the direction and magnitude of misalignment, the component analysed and maybe even the turbine type. It is thus recommended to further investigate this field of study, especially for wind speeds close to rated conditions since the field tests have shown that it is were the larger power gains could be obtained thanks to this WFC strategy.

7 Grid code requirements and provision of power system services

The quality of electric power systems and the stability of the electric power grid depends on manifold parameters driven by he dynamic interaction between connected facilities and consumers. In order to control and maintain grid power quality the grid operators/Transmission System Operators (TSO's) have set up grid codes for their authorised area for all connected facilities and power suppliers. The electrical power quality is typically measured at the point of connection to the electricity grid (PoC). On top of the required grid support activities the connected facilities could provide additional power system services, also often called ancillary services, which are billable and could contribute on wind farm operators energy portfolio.

7.1 Common grid code requirements

7.1.1 Frequency and voltage range

Grid codes specify a frequency range around the nominal grid frequency in which operation of the facility that is to be connected must be viable. This range is regularly divided into an narrower continuous operation range and one or more wider temporary operation range(s). In the continuous range (e.g. $\pm 2\%$), operation must be possible at all times, just like at the nominal frequency. In the temporary range(s) (e.g. $\pm 5\%$), operation must be sustainable for a defined time frame, where if several temporary ranges are defined, the time frame gets shorter with increasing frequency deviations.

Similar to the frequency range, also a voltage range is defined in grid codes. This voltage range is also subdivided into continuous and temporary ranges in an identical way. The only relevant difference is that the voltage tolerances are wider (usually 5-15 %) than frequency tolerances (usually 2-5 %). The reasons for this are that small voltage fluctuations in general are less problematic, while even small frequency fluctuations can be critical for rotating electrical machines, and that keeping a very narrow voltage range is difficult and resource-intensive and therefore costly. Voltage tolerances differ per voltage level, where the tolerance range becomes narrower with increasing voltage levels.

7.1.2 Reactive power capability

Grid codes demand the ability to control reactive power exchange at the point of common coupling (PoC). This capability is usually specified as a function of the grid voltage and the exchanged active power.

With regards to voltage, the usual way of providing reactive power to a network is to produce it when voltage is too low and to consume it while voltage is too high, as this behaviour counteracts voltage deviations and helps to stabilise the voltage at the nominal value. The requirements in grid codes should reflect this beneficial behaviour, but it cannot be taken for granted that all grid codes will. Demanding a fixed reactive power capability, irrespective of the voltage, would also require the possibility of providing reactive power in case of too high voltage, and consuming reactive power in case of too low voltages. These capabilities would have little value for grid operation, and would probably not be used, but they would increase the cost of a wind power plant, as demanding this capability puts higher demands on the electrical equipment. The European grid code framework by ENTSO-E [28] explicitly allows European TSO's to define such requirements.

With regards to active power, it is common to relate the reactive power capability to the actual active power. This avoids the need to provide reactive power in case of zero (or very low) active power, which basically would be operation as a Static Synchronous Compensator (STATCOM). However, the European grid code framework by ENTSO-E explicitly allows European TSO's to require STATCOM capability.

7.1.3 Active power frequency response

Grid codes usually require the capability of active power frequency response, meaning the ability to change the active power output as a predefined function of the locally measured frequency in order to counteract undesired frequency deviations. The subject can be split into over-frequency and under-frequency response.

Over-frequency response is rather easy to achieve (reduction of the power output), it is easily compatible with state-of-the-art wind turbine control, and it is commonly implemented for most generation units, including wind and solar power. Power reduction and curtailment is e.g. achieved by WFC strategies such as axial induction.

Under-frequency response, however, is more challenging as it demands an increase of the power output. It can only be provided if an upward margin is kept, and this implies operating at a lower set-point than what is possible. Since wind power plants usually operate at the maximum power (low wind speed) or at rated wind power (high wind speed), they normally do not have an upward margin to increase power output. Keeping such a margin results in a continuous loss of non-harvested energy, which is undesirable from an economic point of view.

So even though the *capability* to provide under-frequency response is demanded in grid codes, it is not common to *actually use* this capability, to avoid the aforementioned energy loss. However, as electric power systems more towards higher shares of sustainable power sources, the need to utilise the capability and accept the energy losses is steadily increasing. Meanwhile, many wind turbine OEM's have included turbine control features that allow short term power increase around rated wind speed, so called "power boost" features, which could be applied to provide under-frequency response on request. The WFC strategy wake steering is also an appropriate feature that allows short term farm power output increase of several percent as indicated in field tests performed by ENGIE described in Section 5.

Ireland, which has small and almost closed up island grid, is acting as a pioneer, economically compensating wind power plants for providing these power system service. A defined number of on- and offshore wind farms are operating in "stand-by" mode providing back up power in case of unexpected power consumption on the island.

7.1.4 Fault ride through

Fault ride though (FRT) requirements demand from power generators to tolerate short-term grid voltage deviations, and to keep operating. These faults are typically characterised by sudden voltage dips in the range of milliseconds caused e.g. by an external short circuits or a facility power loss. Normally, in such cases the wind turbine converters of each wind turbine would trigger a shut down in order to bring the wind turbine into a safe mode. As a consequence, such continuously shut down chain reactions would lead to an amplification of the system incident and could full electric cause black outs.

While being valid for conventional power stations, wind power was excluded from this requirement in the early days of wind power development, but as this exclusion resulted in threats for power system stability, the requirement was also applied to wind power plants. Today, many wind turbine controls are able to detect such voltage dips and keep the the wind turbine generator connected to the grid, despite a grid instability. This capability is e.g. covered in a Grid Code Compliance Certificate according to DNV-ST-0125 [22]. However, in the instant of an undervoltage FRT the wind turbine rotor experiences extreme transient rotor speed variations resulting in strong drive train vibration and high torsional loading. This load scenario has to be covered and validated by the Type Certificate of the wind turbine.

The cost for the wind power plant are limited, but the benefit for the power system is large. It is therefore a brilliant example of a good grid code requirement.

7.2 Differences between different TSO grid codes

There are may local differences in frequency and voltage ranges, as each TSO can specify them according to his individual preferences and needs. The same applies for the reactive power capability, exhibiting local differences in the characteristics that define the capability as a function of grid voltage and active power.

However, when comming to FRT requirements, the story becomes much more complicated. Considering the commonly known FRT curves (for undervoltage faults), local differences exist, but the curves all share a similar concept. This is, however, only true for single symmetrical undervoltage faults, and only for the specification of the faults voltage deviation and duration that needs to be tolerated. When moving on to symmetric overvoltage faults or asymmetric faults (both over- and undervoltage, or even combined) or sequential faults, there exist no specifications from the European grid code framework by ENTSO-E [28], opening up for large differences between individual TSO grid codes.

The same applies to the actual response to the fault. Neither the behaviour during the fault, nor the post-fault recovery are specified on European level, as large local differences prohibit European harmonisation. While some TSO's prioritise active current, others prioritise reactive current. There are even cases of the absence of behaviour specifications, which jeopardises the concept of FRT, as the demand to remain connected only serves a purpose when some useful behaviours is ensured. Considering post-fault behaviour, some TSO's demand as-fast-as-possible post-fault recovery, while others demand a defined ramp back to normal.

Another topic with significant differences within Europe is the location of the connection point of offshore wind power plants. Some countries (e.g. Germany) define the connection point to be offshore at the location of the power plant, which makes the export cable to shore a part of the transmission grid. Other countries (e.g. England) define the opposite, with the connection point being located onshore and the export cable being part of the power plant. This causes massive differences in the grid code requirements which are to be met at the connection point, as the grid properties are different offshore and onshore.

These differences are challenging for the wind industry and for certification, as the prohibit the possibility for a unified European grid code compliance certificate.

7.3 Power system services

Power system services are all form of grid-supportive behaviour which a grid connected facility can provide to the grid on a voluntary basis. These services are usually paid by the TSO, and can be procured with direct agreements or through markets. Power system services are often seen as the "opposite" of grid code requirements, which define legally binding behaviour which is not voluntary or economically compensated.

There is, however, a significant overlap between grid code requirements and power system services: Grid code requirements can demand the capability to be able to do something. And a system service market can procure and schedule which grid connected facilities actually do it. This separation between obligatory/voluntary and capability/action is very meaningful. To ensure the stability or the electric power system, it is a wise idea to demand minimum capabilities to support grid stability from all connected facilities. However, as making use of these capabilities can imply additional cost to the facility owner, it makes sense to procure the system services through a market, to assure that any service is provided by the facility that can do it at the lowest cost, and to assure that the implied cost are compensated for.

A nice example of the a paid power system service is the provision of fast frequency regulation in Ireland. While the capability to provide active power frequency response is demanded by the Irish grid codes, it is a paid power system service to do so for wind power. And the payment is a function of the response speed, which provides economic incentives for innovation (fast active power control).

7.3.1 Black start requirements and WFC capabilities

Another challenging (and billable) power system service is the capability of a facility to start up independently from the external grid situation. The Requirements for Generators Network Codes [29] defines black start as the capability of a power-generating module to recover from a total shutdown through a dedicated auxiliary power source without any electrical energy supply external to the power-generating facility. With the increase of generation from renewable sources such as offshore wind to meet global climate net zero targets, there are less fossil fuel power plants available in the grid that can provide power system services such as black starting following a partial or major grid blackout. This highlights the need to develop alternate ways to achieve black start capability using renewable sources such as wind farms. The practical feasibility of achieving this is black start service in its entirety from a wind farm is still uncertain being the obvious problem of wind being variable and the required modifications required in the wind farm control system such as the ability to self-start under island mode, and ability to act as a grid forming voltage source to establish the grid network system frequency.

The following subsections summarises the present state of black start services first from an EU regional perspective and then highlights a UK case study of looking at the required changes and adaptations required from wind farm control.

7.3.2 Black Start – ENTSO-E Network Codes

The European network codes (NC) are a set of rules drafted by ENTSO-E, with guidance from the Agency for the Cooperation of Energy Regulators (ACER), to facilitate the harmonisation, integration, and efficiency of the European electricity market. Two network codes govern the implementation of black start also known as Restoration Services.

- Requirements for Generators (RfG): Commission Regulation (EU) 2016/631 of 14 April 2016 establishing a network code on requirements for grid connection of generators [28]

- Emergency and Restoration: Commission Regulation (EU) 2017/2196 of 24 November 2017 establishing a network code on electricity emergency and restoration [29]

The RfG detail the requirements for grid connection of generators such as wind farms while the Emergency and restoration codes establishes processes that transmission operators follow to keep the highest standards and practice in dealing with emergency situations. The objective of both requirements is to guarantee that there is a sufficient amount of generation capable of black start for the power system restoration process after major disturbance or a blackout.

Article 15 (5) (a) of the RfG NC [28], governs power generating module with a black start Capability and states they shall fulfil the following:

- be capable of starting from shut down shutdown without any external electrical energy supply within a time frame specified by the relevant system operator in coordination with the relevant TSO.

- be able to synchronise within the frequency limits laid down in point (a) of Article 13(1) and, where applicable, voltage limits specified by the relevant system operator or in Article 16(2).

- be capable of automatically regulating dips in voltage caused by connection of demand.

- be capable of regulating load connections in block load

- control frequency in case of over-frequency and under-frequency within the whole Active Power output range between Minimum Regulating Level and Maximum Capacity as well as at house load level.

- be capable of parallel operation of a few Power Generating Modules within one island

- control voltage automatically during the system restoration phase

These requirements are more tailored to fossil based generation power plants which are gradually been phased out but are possible to be met by wind farms as well. Therefore, the specific details must be defined locally by the Relevant Network Operator. For example, it will only help during the restoration process when wind is available. Hence, TSO's must analyse the different existing wind farms to be the most suitable for this service and wind turbine manufactures need to modify their existing wind farm control systems to incorporate black start Capability.

7.3.3 Black Start – UK Power System Services

The UK already considers black services as part of a group of balancing power system services for the grid. In its current form, this is provided by large synchronous power stations but with current transition to net zero and the phasing down of coal powered stations, the transmission systems operator National Grid ESO has been creating solutions for what is called 'non-traditional technologies' (e.g., wind power, solar and energy storage) to participate in the black start market [48]. The approach considers a combination of various non-traditional technologies to meet the technical requirements of the different black start stages. The Distributed ReStart project [49] with UK TSO National Grid ESO and DNO SP Energy Networks is currently ongoing looking at a demonstrator trail of how wind, solar and hydro can be used to restore power to the transmission network in the unlikely event of black start.

The capability of wind turbines to self-start in island mode without external power supply requires additional design and control features (e.g. back-up power/battery power supply). They could be certified within the OEM's Type Certificate of the wind turbine.

Existing technical requirements for black start in the UK fundamentally fall into four categories:

- the ability to start up independent of external supplies

- the ability to energise part of the transmission network

- and the ability to block load local demand

- the ability to sustain black start over long durations (3-7days)

Table 7 lists the key technical requirements that must be met by black start providers

Category	Requirement	Definition
Time to connect	≤ 2 h	Time taken to start-up black start plants from shutdown without the use of external power supplies.
Service availability	≥ 90%	Deliver contracted BS service over 90% of a year
Voltage control	±10%	Ability to control voltage within limits (±10%) when block loading
Frequency control	47.5 – 52 Hz	Ability to manage frequency level (47.5 – 52 Hz) when block loading
Resilience of supply (Black Start Service)	≥ 10 h	The minimum time the provider will deliver the contracted service.
Resilience of supply (Auxiliary power)	≥ 72 h	Be able to run continuously at rated output for a minimum of three days
Block loading size	≥ 20 MW	Capability to accept instantaneous loading of demand blocks
Reactive capacity	≥ 100 MVAr for 400/275 kV (or 50 MVAr for 132 kV)	Ability to energise part of the network (MVAr > 0, MW = 0)
Sequential start-up	≥ 3	≥ Able to perform at least 3 sequential start-ups

Table 7: Technical Requirements for black start Power System Services

The current approach in the UK is to select the best technologies suited at different stages of black start. The stages are illustrated in the Figure 22 below.
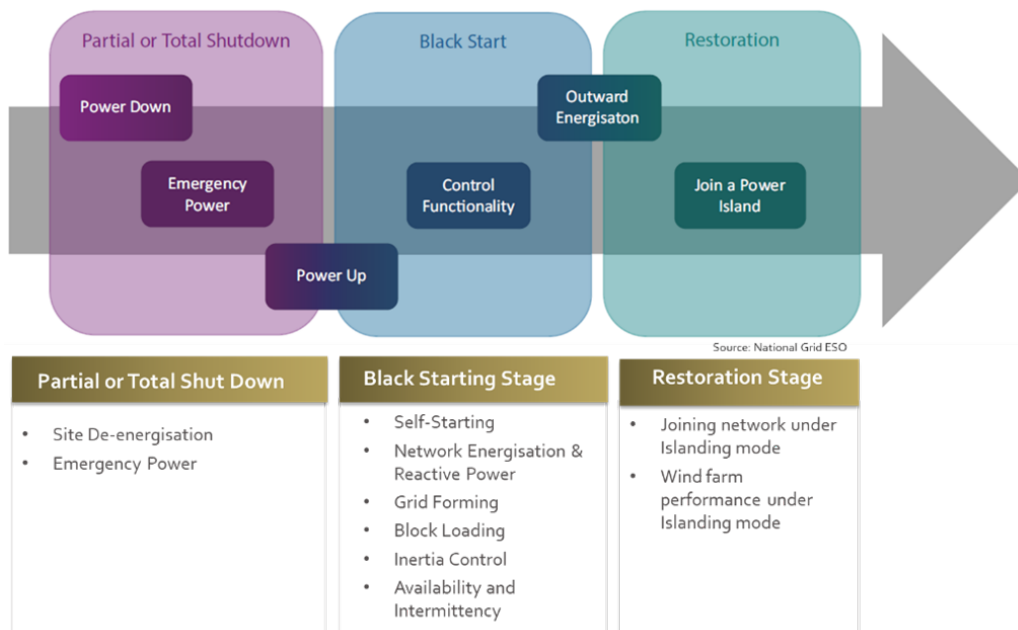
Figure 22: Different stages in a Black Start service

7.4 Challenges with WFC

The application of WFC should at a first glance not lead to problems for grid code compliance assessment. As all grid code requirements are valid at the connection point, any internal behaviour of the wind power plant is neither relevant nor interesting to the TSO. Only the behaviour at the connection point matters. As an example, when reactive power is demanded, it does not matter to the TSO if all wind turbines provide equal shares, or of some provide more than others, or the reactive power is provide by other assets within the wind power plant.

However, challenges might appear if more advanced WFC control methods are used, which rely on Artificial Intelligence (AI), data-driven concepts, or any self learning or adapting methods. With such control in use, it is not deterministic how a wind power plant will behave in a given situation, as the behaviour is not only determined by the situation, but also by the entire history that fed the self-learning process. It is therefore hardly possible to definitely certify grid compliant behaviour, as the behaviour is to some extend unknown.

For general certification of Grid Code Compliance (GCC) the DNV service specification DNV-SE-0124:2021 "Certification of grid code compliance" applies. Corresponding to the sercive specification the standard DNV-ST-0125:2021 "Grid code compliance" [22] contain the scope of certification works. International applicable grid code standards are given in Table 8 and Table 9.

Table 8: Internationally public available Certification Scheme for GCC

Number	Title	Reference
DNV-SE-0124	Certification of grid code compliance	[29]
prEN 50549-10	Requirements for generating plants to be connected in parallel with distribution networks — Part 10: Tests demonstrating compliance of units	[30]

Table 9: Nationally public available Certification Scheme for GCC

Country	Title (translated to English)	Reference
Germany	Technical Guidelines for power-generating units, modules as well as storage and for their components Part 8 (TR8)	[27]
Spain	Technical conformity supervision standard per EU Regulation 2016/631 for power-generating modules (NTS 2.1)	[28]

For further background regarding detailed scope of work of GCC certification modules reference is made to TotalControl report D4.7 [30].

8 Recommendations for updates in certification and standard documents

8.1 Recommendations for certification of design basis

Within a certification process a design basis document is representing the certification schedule comprising the description of the system, list the applied standards, their hierarchy and provides an insight of engineering methodologies that should be further described in design documents. The following list is an extract which might be extended depending on the specific WFC concept:

- Specification of WFC functionalities

- Definition of assets and components used for WFC

- Specification of anticipated operation times in WFC conditions

- Specification of yaw activities related to WFC (wake steering). Definitions of expected yaw offset and expected operation time.

- Specification of pitch activities related to WFC (axial induction). Definitions of expected amplitudes of extra cyclic pitch angles and expected time period for cyclic pitch activities.

8.2 Recommendations for certification of control & protection system

For the certification of the wind turbine control & protection system connected to a WFC system the following additional information should be provided for certification purpose:

- Descriptions of possible malfunctions in the WFC functions and how they can be detected during commissioning of the functions and in the wind farm operation phase (FMEA)

- Interface definitions at wind turbine terminals for communication related to WFC. The wind turbine must be able to both receive and transmit relevant data.

- Wind farm specific definitions of communication interfaces between WPPC (Wind Power Plant Control) and WTC (wind turbine control)*

- Consideration of a sensor for nacelle yaw orientation relative to tower at each wind turbine (absolute nacelle yaw position). This signal is needed for WFFC control.

- The control software at the WPPC should should fulfil the requirements of DNV-ST-0438 "Control and protection systems for wind turbines":2021, section 2.9 (or IEC 61400-1:2019 Editon 4.0 [1]).

- Prove that WFC features fall inside the definitions of wind turbines design specification

- Specifications on measures on cyber security in the communication networks

*The interface between the Wind Power Plant Control (WPPC) and the Wind Farm Flow Control (WFFC) and the challenges regarding communication and internal prioritisation are described more detail in FarmConners report D3.6 "Towards integrated wind farm control: interfacing farm flow and power plant controls" [34].

Regarding Test of Turbine Behaviour the following tests should be added to the test plan.

- Tests to prove the WFC control procedures

- Test to prove the wind direction signal calibration up the angle of maximal yaw misalignment (wind vane)

- Test to prove the wind speed signal calibration up the angle of maximal yaw misalignment (anemometer)

8.3 Recommendations for ILA and design certification

The purpose of the Integrated Load Analysis (ILA) is to examine whether the site-specific loads on the integrated wind turbine structure, including the rotor-nacelle assembly (RNA), support structure and supporting soils, are derived in conformity with the design basis. An ILA will be performed within the Site Specific Design Assessment (SSDA) module of DNV-SE-0190 [18] as part of the project certification.

In Section 5 the capability of wind farm simulation tools has been presented. The fast computation by means of surrogate models are in line with a number of uncertainties for the load prediction. However, such tools are convenient to identify critical positions within a wind farm on a qualitative level.

Therefore, it is recommended to perform prior to a aero-servo-elastic coupled analysis a sensitivity study on wind farm level. Such a sensitivity study could identify critical ULS and FLS positions within the wind farm. As a result the following possibilities for the detailed load simulation exist:

- The sensitivity study reveals that not just single turbines see worst case loads, but an entire region of the wind farm receives exceptional loads.

  -> Division of the wind farm into clusters and simulate all turbines within the highest loaded cluster by fully coupled analysis simulations.

- Just a few turbines appear significantly higher loaded.

  -> Recalculate the identified critical positions by fully coupled analysis.

Alternatively to wind farm simulation tools, the sensitivity analysis on farm level may be performed with existing and widely validated complex terrain simulation tools. The ability for modelling WFC flow conditions in a sufficient way has to be demonstrated. In a later stage, when wind farm simulation tools have passed a significant number of validations and comparisons to full scale measurements it might be possible to determine component loads on wind turbine level directly by farm simulation tools.

In the present development stage of most of the wind farm flow and wake tools the following activities regarding ILA are recommended:

- Include WFC operations in the ILA. One of the reasons for performing the ILA is to prove that wind turbine loads are not exceeding the design loads from wind turbine Type Certification. Thus, by including WFC operations in the ILA it can be shown that the effects from WFC on turbine loading are acceptable

- Define requirements for testing in order to prove WFC measures effectiveness during wind farm operation. The purpose of this testing is to provide related regular reporting within Project Certification in-service phase. Alternatively, monitoring of selected load sensors could be agreed with the certification body.*

*Load measurements on a prototype is a mandatory part of the RNA Type certification [19]. The load measurement procedure for wind turbines is described in the IEC61400-13 standard [4]. Additional WFC Measurement Load Cases (MLC) should be added to the prototype measurement programme during steady-state operation. The WFC strategies and their full extend of setpoint variation should be represented in the MLC's. Subsequently, these measured MLC's should be compared with simulated WFC load cases of the corresponding ILA.

The ILA is based on a predefined set of load cases which are listed in the Design Basis. Load case catalogues for wind turbines are defined in the Standards by IEC and DNV. The application of a complete load case catalogue is a mandatory requirement to achieve a Type Certificate (wind turbine) or a SSDA (wind farm). In the following the application range of current load case catalogues is illustrated.

Table 10: Standards including ILA load case catalogues

Standard	Application	Load case table No.
IEC 61400-1:2019	Onshore	Table 2 and Table B.1
IEC 61400-3-1:2019	Offshore	Table 2
IEC 61400-3-2:2019	Floating	Table 2
DNV-ST-0437:2021	Onshore + Offshore	Table 4-3 and Table 4-4
DNV-ST-0119:2021	Floating	Table 4-4

Based on the simulation results presented in Section 4 and 5, and on the field experiences reported in Section 6, it appears reasonable to combine the existing load case catalogues with respective WFFC activities, rather than create new, special WFFC load cases. Therefore, the following WFFC load case descriptions is orientated on the existing load case catalogues of IEC and DNV. This table might serve as discussion basis for future standard updates.

DLC + wind model	Comments with respect to WFFC	Type of analysis
DLC1.1 NTM	Probabilities of occurrence to be considered for extrapolation	U for extrapolation
DLC1.2 NTM	Probabilities of occurrence to be considered for fatigue weighting	F / U*
DLC1.3 ETM	case 1: ETM without WFFC, case 2: ETM with WFFC	U
DLC1.4 ECD	case 1: ECD without WFFC, case 2: ECD with WFFC	U
DLC1.5 EWS	case 1: EWS without WFFC, case 2: EWS with WFFC	U
DLC2.1 NTM	based on FMEA for WFFC	U
DLC2.2 NTM	based on FMEA for WFFC	U
DLC2.3 EOG / NTM	case 1: EOG without WFFC, case 2: EOG with WFFC	U
DLC2.4 NTM	superposition of WFFC (e.g. wake steering) and additional yaw offset demand may require special attention also for the fatigue loads	F / U*
DLC2.5 NWP	DLCs considering UVRT (formerly LVRT), in combination with WFC	U
DLC3.1 NWP	depends on WFC strategy	F / U *
DLC3.2 EOG / ETM	see above for DLC3.1 or case 1: EOG without WFFC, case 2: EOG with WFFC	U
DLC3.3 EDC	see above for DLC3.1 or case 1: EDC without WFFC, case 2: EDC with WFFC	U
DLC4.1 NWP	depends on WFC strategy	F / U *
DLC4.2 EOG / ETM	see above for DLC4.1 or case 1: EOG without WFFC, case 2: EOG with WFFC	U
DLC 5.1 NTM	superposition of emergency-stop and WFFC at NTM	U
DLC6.1 EWM	depends on WFC strategy	U
DLC6.2 EWM	depends on WFC strategy	U
DLC6.3 EWM	depends on WFC strategy	U
DLC6.4 NTM	depends on WFC strategy	F / U *

DLC + wind model	Comments with respect to WFFC	Type of analysis
DLC7.1 EWM	depends on WFC strategy	U
DLC8.1 NTM	depends on WFC strategy	U
DLC8.2 NTM	depends on WFC strategy	U

* Type of analysis U for these DLC's is not listed in IEC 61400-1:2019, Table 2, but any fatigue load case needs also to be evaluated for extreme loads.

9 Conclusion

This report completes the research work started with the position paper on certification and standardisation in the begin of the FarmConners research project, issued in July 2020 [35]. The collaborative research activities of the different Farm-Conners work packages contributed with new insights, new findings, new tool developments and important measurement data to the updated recommendations for certification and standardisation of Wind Farm Control (WFC).

Work package 1 provided testing and validation of of WFC strategies on full scale wind turbines and wind farms and demonstrated in the potential of WFC to improve energy output of wind farms on real assets. Furthermore, the development and improvement of high fidelity simulation tools, supported by wind tunnel tests and field measurements provided a boost of confidence in the numerical prediction of farm flow conditions under complex operating conditions. In work package 2 comprehensive sensitivity studies on the loading effects due to WFC strategies and Wind Farm Flow Control (WFFC) in particular have been performed. They completed a picture of WFC control impacts on the win and loss side. Finally, work package 3 brought in the economic aspects of WFC and the new developments and opportunities in the European electricity market for renewable Wind Power Plants (WPP). Here the requirements of the TSO's and the interface with new optimised wind farm outputs contributed to the development of certification and standardisation proposals on the grid side.

The most common WFC strategies currently under investigation are considered in this report, comprising

- axial induction (power curtailment of upwind turbines) and

- wake steering (operating under high yaw misalignment angles).

Here the wake mixing strategy, a low frequency thrust pulsing approach, is considered as part of the axial induction concept.

Two simulation packages have been analysed. First, a sensitivity study on turbine level looking at combined WFC activity and simultaneous extreme events, and secondly, a flow simulation on farm level of WFC load effects with focus on fatigue loading. Both surveys revealed that there are some draw backs in line with the desired improved power performance. Potential risks have been identified which doubtless showed overloading of specific turbine components due to active WFC strategies in ultimate limit state and fatigue limit state as well.

It turned out that the wake steering strategy is responsible for the dominant loading surplus on wind turbine components. Under large yaw misalignment angles up to 30° the extreme loads for the rotor-nacelle (RNA) components increased between +10% to +40% (calculated with a DTU 10MW reference model). Fatigue load simulations on farm level of the Lillgrund wind farm (DK) applying a power optimised wake steering strategy delivered an increases of up to +30% of damage equivalent loads at the blade roots and up to +20% at the tower bottoms. On the other hand these higher load levels have been the price for a remarkable power performance plus of +7%. Furthermore, the simulated load effects found in both numerical simulations could be confirmed qualitatively by field measurements in the French wind farm La Sole du Moulin Vieux, performed during the FarmConners project.

The review of the simulations executed in this project made clear that the capture of wind farm flow and wake effects in a reasonable accuracy is a challenging task and the various numerical approaches available reach quickly limits of today's computational capacities and acceptable simulation times. The current achievable accuracy in the load prediction under complex wake conditions, especially fatigue loads, does not satisfy the expectations and needs of the wind industry. Therefore, it is recommended to apply the presented tools for qualitative analysis and the identification of most severe loaded locations within a wind farm. The identified locations could be then analysed in detail by classic aero-servo-elastic codes in a coupled analysis.

However, with further progressing development and validation of the existing wind farm simulation tools by field experiences it is foreseen that these tools could be applied in the near future by the industry for design works and by certification bodies for verification. Here the surrogate model approach appeared very promising in terms of accuracy and speed performance.

The possibilities of WFC to run a wind farm like a power plant enables additional opportunities in providing power system services. Beside the fulfilment of standard power quality requirements, defined by local grid codes, WFC allows to provide additional (and billable) grid supporting services. Beside short term power derating (e.g. by axial induction) or fast power increase on demand (e.g. by wake steering), black start capabilities could be a further attractive extensions of wind farm portfolios. However, it should be ensured that the minimum grid code requirements and Fault Ride Through (FRT) functionalities are maintained at all possible WFC operation modes. This could be checked and confirmed by a third party certification, e.g. with a Grid Code Compliance (GCC) certification.

As a consequence of the performed research activities certification of WFC strategies, either in the wind farm development phase or during a post installation retrofit programme, appears necessary in order to identify unexpected overloading effects and to assure operation within given design margins. This check could be implemented by the OEM already during the RNA design. The integrated WFC design of the RNA could be confirmed by the RNA Type Certificate, indicating that the machine is ready for WFC (within clearly defined operational margins). Alternatively, the installation of WFC in an existing wind farm could be accompanied by a certification body by performing an update of the Site Specific Design Assessment (SSDA), taken the local environmental conditions and the specific WFC strategies of the wind farm into account.

Both certification approaches already exist for standard wind farm controls and have to be extended now for WFC application. This report provides a set of recommendations for the extended documentation required for the certification of WFC (amendments to the certification design basis). Requirements for the control & protection system on wind turbine level are also formulated. The hard wired safety chain of the individual wind turbine shall be kept at highest priority. In case of communication errors or WFC functionality faults a fall back to the turbine's normal operation mode shall be possible at any time.

Finally, an amended load case table is introduced including suggestions for consideration of WFC in future standard updates. It has been concluded not to define additional, special WFC load cases but add WFC activities corresponding to their time of occurrence to the existing load case catalogues of IEC and DNV instead. A prerequisite is that the localisation of the most severe loaded turbines within the entire wind farm has been performed in advance, e.g. with the simulation tools presented in this report. This would lead to some extend to much more computational effort compared to classic load simulations, on the designer side and on certification side as well. Nevertheless, it is considered that the proposed calculation process is feasible and practical with the already existing software packages at hand.

Concluding the results and knowledge gained during this project it became evident that the most common WFC strategies are certifiable and existing uncertainties could be mitigated by either comprehensive simulations and/or by accompanied monitoring measures. The lack of clear certification guidance in the present wind turbine standards will be closed soon. In the wind industry the most accepted standards are the IEC or DNV standard. At least DNV plans to update their load standard DNV-ST-437 within 2022 and a detailed section on WFC is already scheduled.

References

[1] IEC61400-1:2019 Edition 4.0. *Wind energy generation systems - Part 1: Design requirements*, 2019. https://www.iec.ch.

[2] Crespo A. *Experimental validation of the UPM computer code to calculate wind turbine wakes and comparison with other models*. *Journal of Wind Engineering, Ind. Aerodynamics, vol. 27, p. 77-88*, 1988.

[3] Tanvir Ahmad, Olivier Coupiac, Arthur Petit, Sophie Guignard, Nicholas Girard, Behzad Kazemtabrizi, and Peter Matthews. *Field Implementation and Trial of Coordinated Control of Wind Farms*. *IEEE Transactions on Sustainable Energy*, 2017.

[4] IEC 61400-13:2016 amendment A1:2022. *Wind turbines - Part 13: Measurement of mechanical loads*, February 2022. https://www.iec.ch.

[5] Maronga B. *The Parallelized Large-Eddy Simulation Model (PALM) version 4.0 for atmopheric and oceanic flows: model formulation, recent developments, and future perspectives*. *Geoscientific Model Development, vol. 8, p. 2515-2551*, 2015.

[6] O.A. Bachau. *Flexible Multibody Dynamics*. In Springer Netherlands, editor, *Solid Mechanics and its Applications*. 2011.

[7] O.A. Bachau, C.L. Bottasso, and L. Trainelli. *Robust integration schemes for flexible multibody systems*. *Comput. Meth. Appl. Mech. Eng.*, pages 395–420, 2003.

[8] C. Bak, F. Zahle, R. Bitsche, T. Kim, A. Yde, L.C Henriksen, and M.H. Natarajan, A.and Hansen. *Description of the DTU 10 MW Reference Wind Turbine*. Technical report, DTU Wind Energy Report-I-0092, 2013.

[9] Bottasso C.L. Bortolotti, P. and A. Croce. *Combined preliminary-detailed design of wind turbines*. *Wind Energ. Sci.*, pages 71–88, 2016.

[10] P. Bortolotti, H. Canet, K. Dykes, L. Sethuraman, D. Verelst, and F. Zahle. *IEA Wind TCP Task 37: Systems Engineering in Wind Energy - WP2.1: Reference Wind Turbines*. Technical report, 2019.

[11] C.L. Bottasso, A. Croce, Y. Nam, and C.E.D. Riboldi. *Power curve tracking in the presence of a tip speed contraint*. *Renewable Energy*, pages 1–12, 2012.

[12] C.L. Bottasso, A. Croce, B. Savini, W. Sirchi, and L. Trinelli. *Aero-servo-elastic modeling and control of wind turbines using finite-element multibody procedures*. *Multibody Syst. Dyn.*, pages 291–308, 2006.

[13] W. Collier and J.M. Sanz. *Comparison of linear and non-linear blade model predictions in Bladed to measurement data from GE 6MW wind turbine*. *Journal of Physics: Conference Series*, The Science of Making Torque from Wind (TORQUE)(753 (2016) 082004), 201.

[14] Rick Damiani, Scott Dana, Jennifer Annoni, Paul Fleming, Jason Roadman, Jeroen van Dam, and Katherine Dykes. *Assessment of wind turbine component loads under yaw-offset conditions*. *Wind Energy Science*, 3(1):173–189, 2018.

[15] Garrad Hassan Partners Ltd. DNV. *Bladed Theory Manual Version 4.8*, 2016. https://www.dnv.com/services/wind-turbine-design-software-bladed-3775.

[16] DNV-RP-A203. *Technology qualification - DNV Recommended Practice*, September 2021. https://rules.dnv.com/servicedocuments/dnv/#!/industry.

[17] DNV-SE-0160. *Technology qualification management and verification - DNV Service specification*, September 2021. https://rules.dnv.com/servicedocuments/dnv/#!/industry.

[18] DNV-SE-0190. *Project certification of wind power plants*, September 2020. https://rules.dnv.com/servicedocuments/dnv/#!/industry.

[19] DNV-SE-0441. *Type and component certification of wind turbines - DNV Service Specification*, September 2021. https://rules.dnv.com/servicedocuments/dnv/#!/industry.

[20] DNV-SE-0474. *Risk based verification - DNV Service specification*, October 2021. https://rules.dnv.com/servicedocuments/dnv/#!/industry.

[21] DNV-SE-0477. *Risk based verification of offshore structures - DNV Service specification*, October 2021. https://rules.dnv.com/servicedocuments/dnv/#!/industry.

[22] DNV-ST-0125. *Grid code compliance - DNV Standard*, November 2021. https://rules.dnv.com/servicedocuments/dnv/#!/industry.

[23] DNV-ST-0437. *Loads and site conditions for wind turbines - DNV Service specification*, November 2016. https://rules.dnv.com/servicedocuments/dnv/#!/industry.

[24] Thomas Duc. *Optimization of wind farm power production using innovative control strategies*. Master's thesis, Technical University of Denmark, 2017.

[25] Thomas Duc. *Optimization of wind farm power production using an axial-induction control strategy: field test results*. SMARTEOLE colloquium, August 28-30, 2018 Orléans, 2018.

[26] Thomas Duc, Olivier Coupiac, Nicolas Girard, Gregor Giebel, and Tuhfe Göçmen. *Local turbulence parameterization improves the Jensen wake model and its implementation for power optimization of an operating wind farm*. *Wind Energy Science*, 4(2):287–302, 2019.

[27] Haibach E. *Betriebsfestigkeit - Verfahren und Daten zur Bauteilberechnungl*. VDI-Verlag Düsseldorf, 1989.

[28] European Network of Transmission System Operators for Electricity ENTSO-E. *The Network Code on Requirements for Generators*, April 2016. https://www.entsoe.eu/network_codes/rfg/.

[29] European Network of Transmission System Operators for Electricity ENTSO-E. *The Network Code on Electricity Emergency and Restoration*, November 2017. https://www.entsoe.eu/network_codes/er/.

[30] Freudenreich K. et al. *Design guidelines and standards*. Technical Report TotalControl Deliverable D4.7, January 2022. https://www.totalcontrolproject.eu/dissemination-activities/public-deliverables.

[31] Gebraad P. et al. *Wind plant power optimization through yaw control using a parameteric model for wake effects -a CFD simulation study*. *Wind Energy, vol. 19, p. 95-114*, 2016.

[32] Jiménez Á. et al. *Application of a LES technique to characterize the wake deflection of a wind turbine in yaw*. *Wind Energy, vol. 13, p. 559-572*, 2009.

[33] Katic I. et al. *A simple model for cluster efficiency*. *European Wind Energy Association conference and Exhibition*, 1986.

[34] Kölle K. et al. *Towards integrated wind farm control: interfacing farm flow and power plant controls*. *FarmConners Delivereable D3.6*, 2022.

[35] Manjock et al. *Position paper on recommendations for certification and standardisation of Wind Farm Control*. Technical Report FarmConners Deliverable D2.1, December 2021. `https://www.windfarmcontrol.info/-/media/sites/windfarmcontrol/publications`.

[36] Natarajen A. et al. *Advanced integrated supervisory and wind turbine control for optimal operation of large Wind Power Plants*. Technical Report TotalControl Deliverable D2.3, 2021. `https://www.totalcontrolproject.eu/dissemination-activities/public-deliverables`.

[37] Paul Fleming. *Wind Farm Controls Research at NREL*. SMARTEOLE colloquium, August 28-30, 2018 Orléans, 2018.

[38] IECRE-OD-502. *IEC System for Certification to Standards relating to Equipment for use in Renewable Energy applications (IECRE System)- Project Certification Scheme Edition 1.0*, October 2018. `https://www.iec.ch`.

[39] Jonkman J. *Development of FAST.Farm: A New Multiphysics Engineering Tool for Wind Farm Design and Analysis*. *AIAA Scitech 2017 Forum*, 2017.

[40] B.J. Jonkman and L. Kilcher. *TurbSim User's Guide: Veresion 1.06.00*. Technical report, NREL Technical Report, 2012.

[41] Stoyan Kamenov Kanev and FJ Savenije. *Active wake control: loads trends*. Technical report, Energy research Center of the Netherlands, 2015.

[42] Knud A Kragh and Morten H Hansen. *Load alleviation of wind turbines by yaw misalignment*. *Wind Energy*, 17(7):971–982, 2014.

[43] Martínez-Tossas L.A. *Large Eddy Simulation of the flow past wind turbines: actuator line and disk modeling*. *Wind Energy, vol. 18, p. 1047-1060*, 2014.

[44] Calaf M. *Large eddy simulation study of fully developed wind-turbine array boundary layers*. *Physics of Fluids, Vols. 22, 015110*, 2010.

[45] Churchfield M. *A large-eddy simulation of wind-plant aerodynamics*. *Proceedings of the AIAA Aerospace Sciences Meeting, Nashville*, 2012.

[46] Jensen N. *A note on wind generator interaction*. *Risoe-M-2411*, 1983.

[47] Troldborg N. *Actuator Line Modeling of Wind Turbine Wakes*. *PhD Thesis, Technical University of Denmark*, 2008.

[48] NGESO. *Black Start from Non-traditional Generation Technologies*, cited 17th January 2022. `https://www.nationalgrideso.com/document/148201/download`.

[49] NGESO. *The Distributed Restart project*, cited 17th January 2022. `https://www.nationalgrideso.com/future-energy/projects/distributed-restart`.

[50] Sørensen N.N. *General Purpose Flow Solver Applied to Flow over Hills*. *PhD thesis, Technical University of Denmark*, 1995.

[51] Fleming P.A. *Evaluating techniques for redirecting turbine wakes using SOWFA*. *Renewable Energy, vol. 70, p. 211-218*, 2014.

[52] Fleming P.A. *Detailed field test of yaw-based wake steering*. *Journal of Physics: Conference Series 753 (2016) 052003*, 2016.

[53] R. Ruisi, E. Bossanyi, and et al. *Wind Farm Control:The Route to Bankability*, 2021. `https://www.dnv.com/publications/wind-farm-control-198162`.

[54] Boersma S. *A control-oriented dynamic wind farm flow model: WFSim*. *Journal of Physics, Conference Series 753*, 2016.

[55] B. Schmidt, J. King, G.C. Larsen, and T.J. Larsen. *Load validation and comparison versus certification approaches of the Risø Dynamic Wake Meandering model implementation in GH Bladed*. EWEA Conference Proceedings, 2011.

[56] E. Simley, P. Fleming, N. Girard, L. Alloin, E. Godefroy, and T. Duc. *Results from a wake-steering experiment at a commercial wind plant: investigating the wind speed dependence of wake-steering performance*. *Wind Energy Science*, 6(6):1427–1453, 2021.

[57] Federico Tagliatti. *Investigation of Wind Turbine Fatigue Loads under Wind Farm Control: Analysis of Field Measurements*. Master's thesis, Technical University of Denmark, 2019.

Appendix A

List of Tables

List of Figures